

HOME

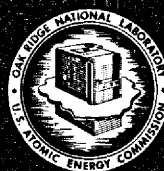
ORNL-TM-4079

HELP

21,003

FORCED-CONVECTION
HEAT-TRANSFER MEASUREMENTS WITH
A MOLTEN FLUORIDE SALT MIXTURE
FLOWING IN A SMOOTH TUBE

J. W. Cooke
B. Cox



OAK RIDGE NATIONAL LABORATORY
OPERATED BY UNION CARBIDE CORPORATION • FOR THE U.S. ATOMIC ENERGY COMMISSION

This report was prepared as an account of work sponsored by the United States Government. Neither the United States nor the United States Atomic Energy Commission, nor any of their employees, nor any of their contractors, subcontractors, or their employees, makes any warranty, express or implied, or assumes any legal liability or responsibility for the accuracy, completeness or usefulness of any information, apparatus, product or process disclosed, or represents that its use would not infringe privately owned rights.

Contract No. W-7405-eng-26

Reactor Division

FORCED-CONVECTION HEAT-TRANSFER MEASUREMENTS WITH A MOLTEN
FLUORIDE SALT MIXTURE FLOWING IN A SMOOTH TUBE

J. W. Cooke

B. Cox

NOTICE

This report was prepared as an account of work sponsored by the United States Government. Neither the United States nor the United States Atomic Energy Commission, nor any of their employees, nor any of their contractors, subcontractors, or their employees, makes any warranty, express or implied, or assumes any legal liability or responsibility for the accuracy, completeness or usefulness of any information, apparatus, product or process disclosed, or represents that its use would not infringe privately owned rights.

MARCH 1973

OAK RIDGE NATIONAL LABORATORY
Oak Ridge, Tennessee 37830
operated by
UNION CARBIDE CORPORATION
for the
U. S. ATOMIC ENERGY COMMISSION

MASTER

C

C

CONTENTS

	<u>Page</u>
Abstract	1
Introduction	1
Description of the Apparatus	2
Operating Procedures	11
Calculations	15
Results	16
Discussion	24
Conclusions	27
Acknowledgments	27
References	27
Appendix A - Additional Details of the Experimental System	29
Appendix B - Experimental Data	37
Appendix C - Computer Program	43
Appendix D - Chemical Analyses and Physical Properties of the Salt	55

C

C

FORCED-CONVECTION HEAT-TRANSFER MEASUREMENTS WITH A MOLTEN
FLUORIDE SALT MIXTURE FLOWING IN A SMOOTH TUBE

J. W. Cooke
B. Cox

ABSTRACT

Heat-transfer coefficients were determined experimentally for a proposed MSBR fuel salt ($\text{LiF}-\text{BeF}_2-\text{ThF}_4-\text{UF}_4$; 67.5-20.0-12.0-0.5 mole %) flowing by forced convection through a 0.18-in.-ID horizontal, circular tube for the following range of variables:

Reynolds modulus	400 - 30,600
Prandtl modulus	4 - 14
Average fluid temperature ($^{\circ}\text{F}$)	1050 - 1550
Heat flux ($\text{Btu/hr}\cdot\text{ft}^2$)	22,000 - 560,000

Within these ranges, the heat-transfer coefficient was found to vary from 320 up to 6900 $\text{Btu/hr}\cdot\text{ft}^2\cdot^{\circ}\text{F}$ (Nusselt modulus of 6.5 to 138). Correlations of the experimental data resulted in the equations:

$$N_{\text{Nu}} = 1.89 [N_{\text{Re}} N_{\text{Pr}} (D/L)]^{0.33} (\mu/\mu_s)^{0.14} ,$$

with an average absolute deviation of 6.6% for $N_{\text{Re}} < 1000$;

$$N_{\text{Nu}} = 0.107 (N_{\text{Re}}^{2/3} - 135) N_{\text{Pr}}^{1/3} (\mu/\mu_s)^{0.14} ,$$

with an average absolute deviation of 4.1% for $3500 < N_{\text{Re}} < 12,000$;
and

$$N_{\text{Nu}} = 0.0234 N_{\text{Re}}^{0.8} N_{\text{Pr}}^{1/3} (\mu/\mu_s)^{0.14} ,$$

with an average absolute deviation of 6.2% for $N_{\text{Re}} > 12,000$.

Keywords: Heat transfer, fused salts, forced convection, heat exchangers, fluid flow, correlations.

INTRODUCTION

The design of molten salt reactors requires detailed information about the transport properties of the proposed fuel, coolant and blanket mixtures. Although the molten salts generally behave as normal fluids with respect to heat transfer,^{1,2} the possibility of unexpected effects,

such as nonwetting of metallic surfaces or the formation of low-conductance surface films, indicates that heat-transfer measurements for specific reactor salts are needed.³ This report describes heat-transfer experiments with a proposed reactor fuel of mixed fluoride salts ($\text{LiF}-\text{BeF}_2\text{ThF}_4-\text{UF}_4$; 67.5-20.0-12.0-0.5 mole %). The technique employs forced convection of the liquid salts through a smooth thin-walled Hastelloy N tube. Resistance heating supplies the tube with a uniform heat flux. This method is particularly well suited to the molten salt system because the electrical resistance of the molten salt is very large compared with that of the metal tube. Furthermore, the resistance of Hastelloy N remains nearly constant over the entire temperature range of the measurements, which simplifies the achievement of an axially uniform heat flux. In addition, a constant heat capacity of the molten salt in the observed temperature range makes possible several convenient assumptions in the calculation of local fluid bulk temperatures.

DESCRIPTION OF THE APPARATUS

The apparatus for studying heat transfer with the molten salt system is shown schematically in Fig. 1 and in the photograph, Fig. 2. Molten salt flows by means of gas pressure through a small diameter, electrically heated test section. The flow of molten salt alternates in direction as pressure from an inert gas supply is added to either of two storage vessels located at each end of the test channel. Each 6-gal salt reservoir is suspended from a weigh cell whose recorded signal indicates the flow rate. The flow of salt reverses automatically by the action of solenoid valves that control the flow of inert gas to the reservoirs. The rate of flow of the salt may be varied from 0.25 to 1.7 gal/min, emptying a reservoir in from 3 to 20 minutes.

The weigh cell circuit shown in Fig. 3 illustrates the electrical and mechanical systems that control the flow of gas and thereby the flow of molten salt. A second suspension system maintains tension on the test section, to prevent it from sagging, by means of counter weights connected by flexible cables. The test section consists of a smooth Hastelloy N tube, 24.5 in. long, 0.25-in. outside diameter, and 0.035-in.-wall

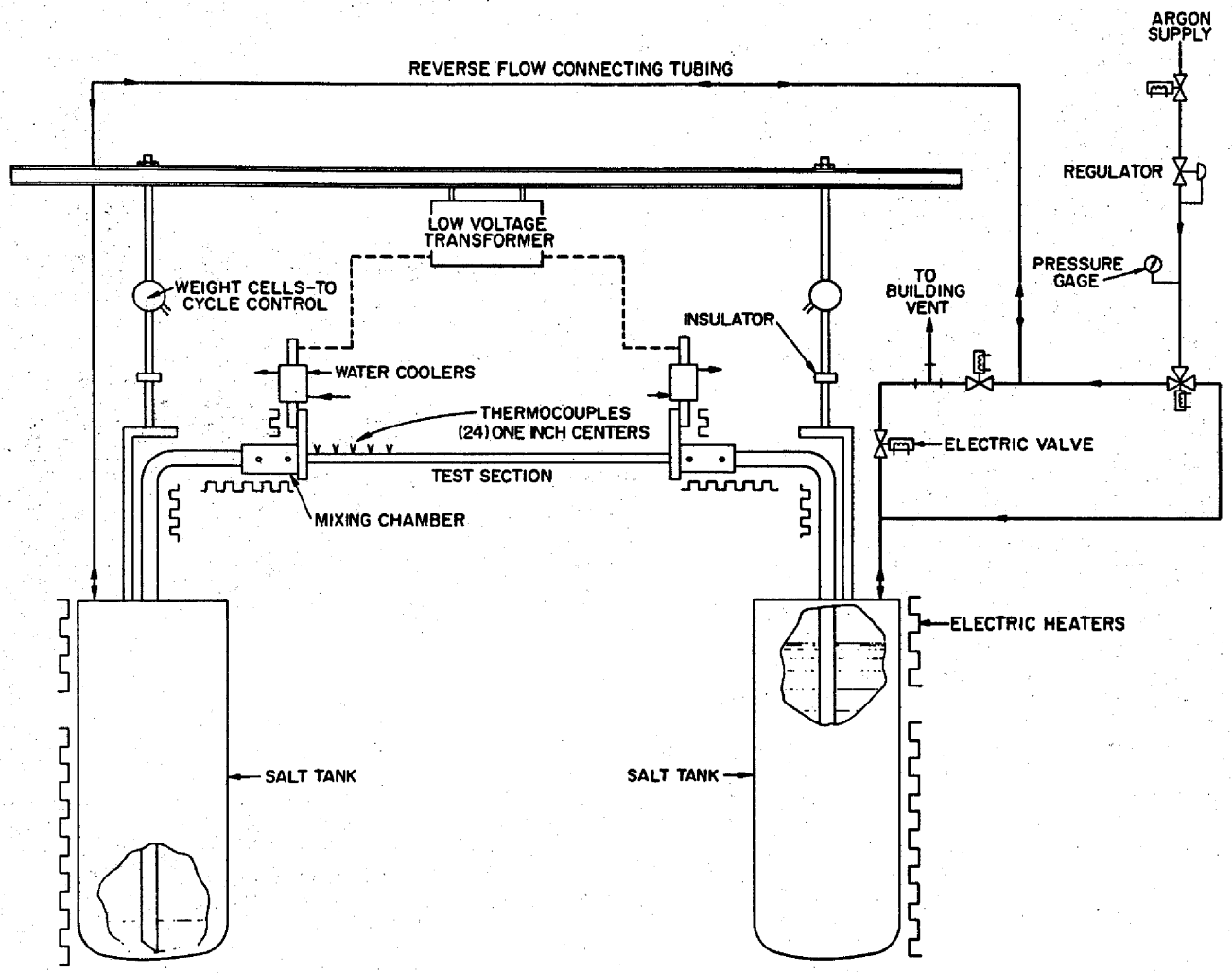


Fig. 1. Schematic diagram for determining the heat-transfer characteristics of molten salt by forced convection.

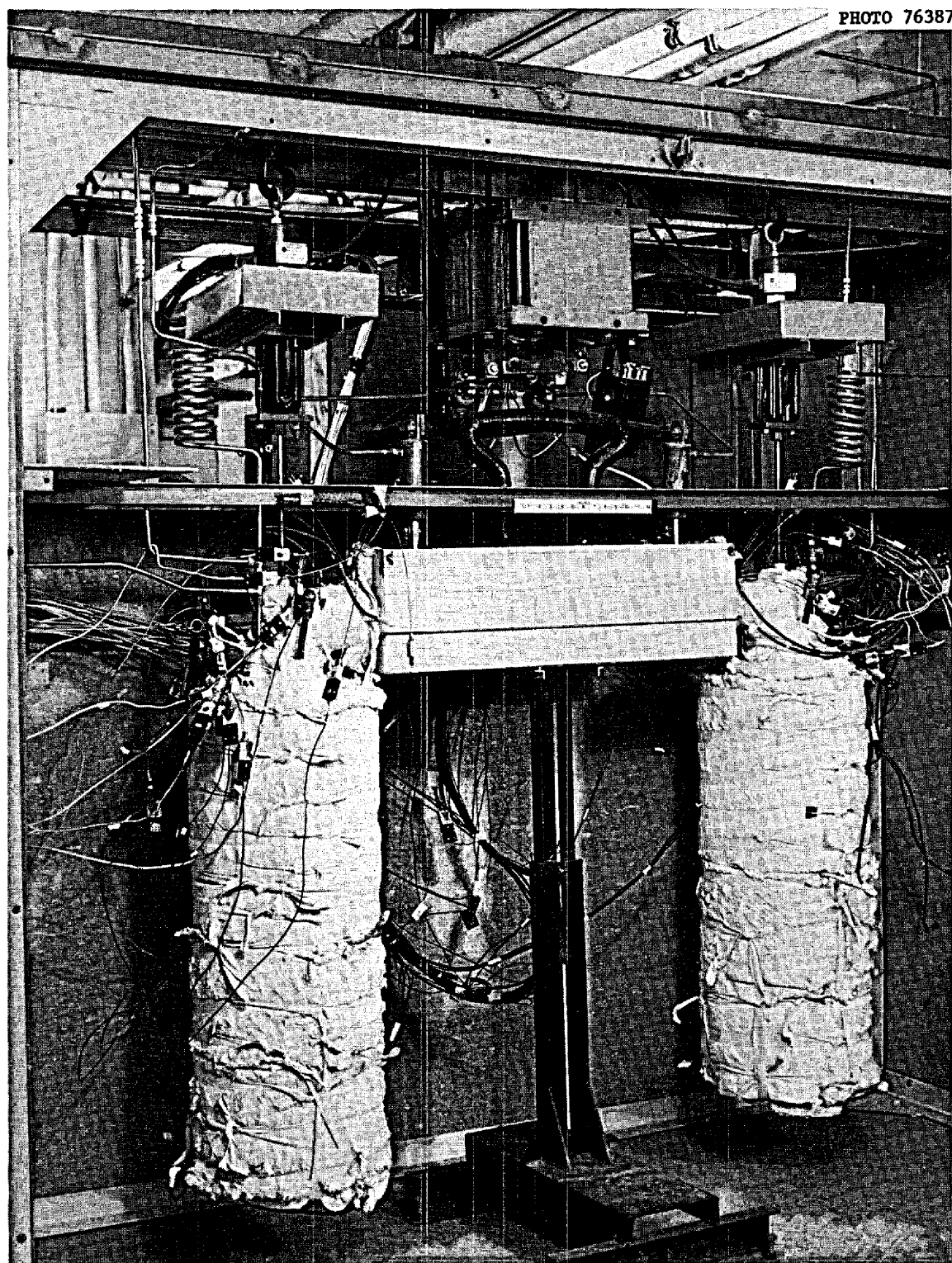


Fig. 2. Photograph of the apparatus viewed from the same aspect as that of Fig. 1.

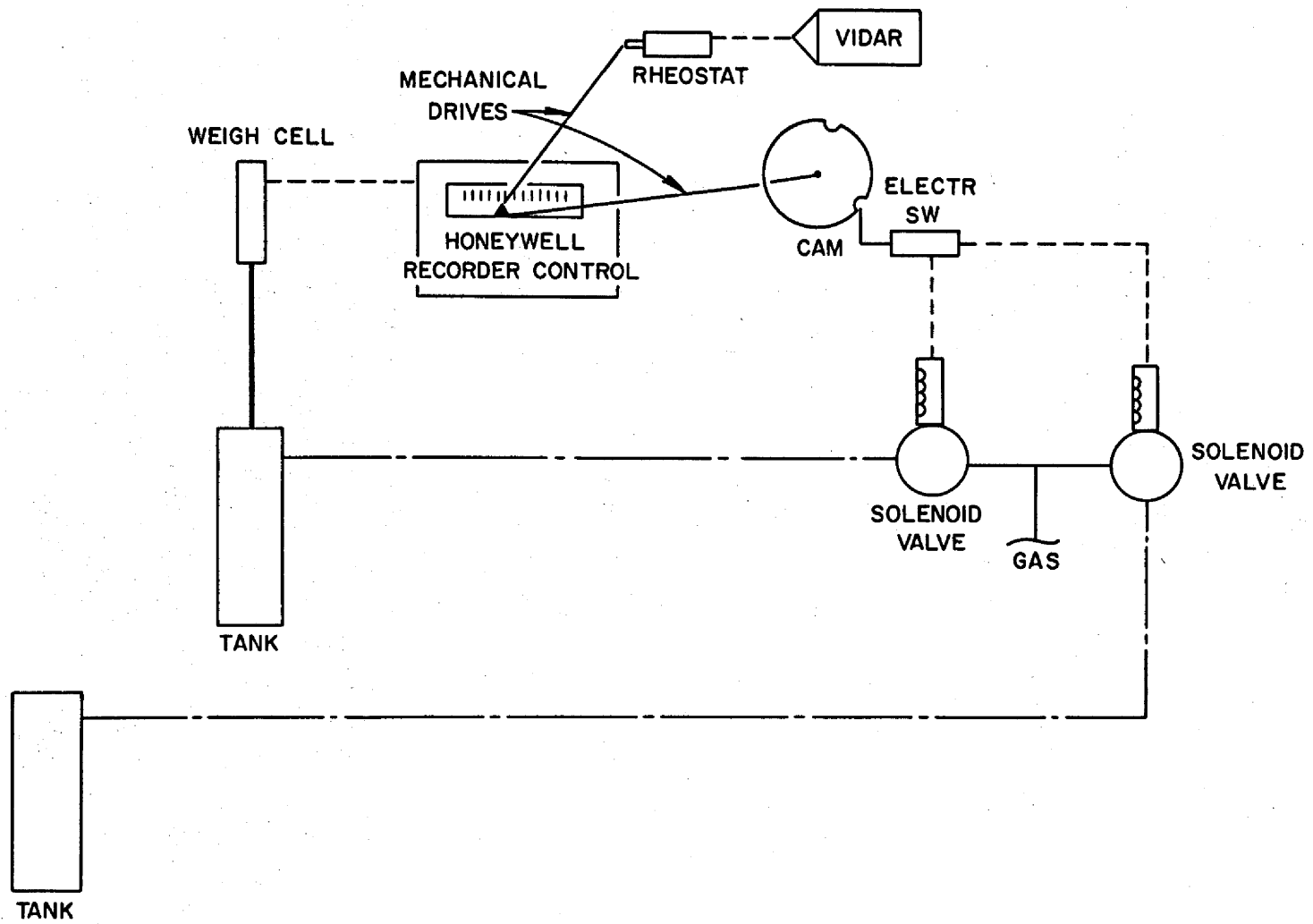


Fig. 3. Weigh cell circuit for molten salt heat-transfer system.

thickness and is resistance heated with a 60 Hz ac power supply. A detail of the mixing chambers located at each end of the test section is shown in Fig. A-1, Appendix A. The electrodes connecting the test section with the power circuit serve also as end plates of the disk-and-donut mixing chambers. The power circuit to the test section is shown in Fig. 4. The electrical power to the test section is supplied by a 440/25 v, 25 kva transformer and is measured with a General Electric watt transducer, also shown in Fig. 4. The test section is insulated with a 3-in.-thick layer of vermiculite powder contained in a sheet metal tray. The salt reservoirs and connecting tubes are heated by auxiliary clamshell and Calrod heaters placed in positions indicated in Fig. 1. A typical heater circuit for an auxiliary heater is depicted in Fig. 5.

The inlet and outlet salt temperatures are measured by four, 40-mil-diam, Chromel-Alumel sheathed thermocouples inserted into two wells in each mixing chamber (Fig. A-1). The temperature distribution along the test section is measured by a series of 24 Chromel-Alumel thermocouples (0.005-in.-diam wire) spot welded at 1-in. intervals to the outside tube wall. The scheme for attaching these thermocouples is shown in Fig. A-2.

Details of a salt reservoir can be seen in Fig. A-3. The interior of these tanks as well as the test section and the mixing chambers are stress relieved and hydrogen fired before they are assembled.

A data acquisition system provides for the automatic monitoring of the temperatures; record is made by a paper printout and a paper tape punch. In this system a multichannel Vidar data recorder reads emf signals from each thermocouple, from the weigh cells, and from the power circuit in a sequential switching arrangement known as a "crossbar scanner." The manufacturer claims an accuracy of better than $\pm 0.5^{\circ}\text{F}$ for the Vidar system. The data recording equipment is shown schematically in Fig. 6 and in a photograph in Fig. 7.

The weigh cell and wattmeter calibration curves and a list of pertinent experimental equipment may be found in Appendix A as Fig. A-4, Fig. A-5, and Table A-1, respectively.

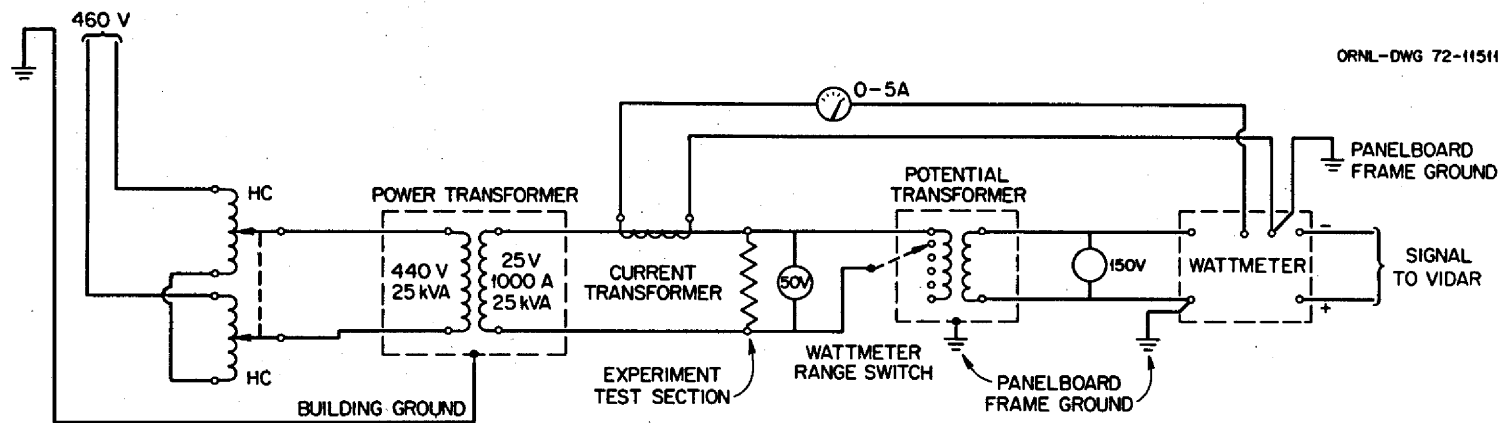


Fig. 4. Test-section power circuit for molten salt heat-transfer experiment.

ORNL-DWG 72-11512

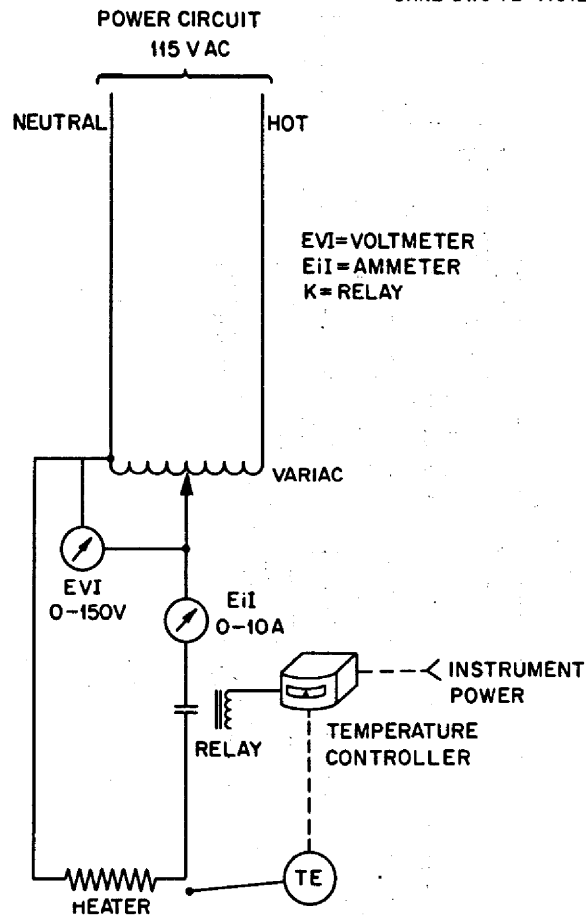


Fig. 5. Typical heater circuit for molten salt heat-transfer experiments.

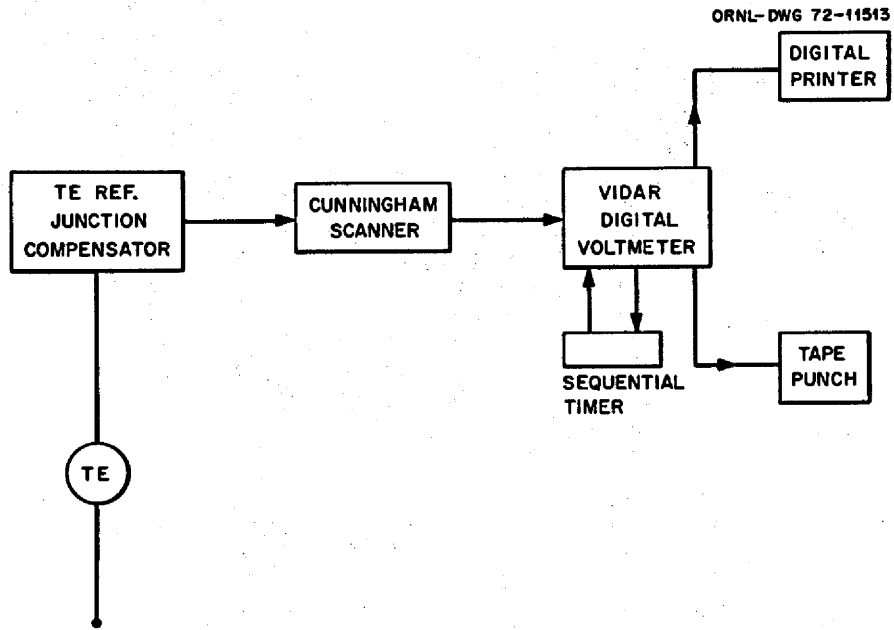


Fig. 6. Thermocouple circuit for molten salt heat-transfer system.

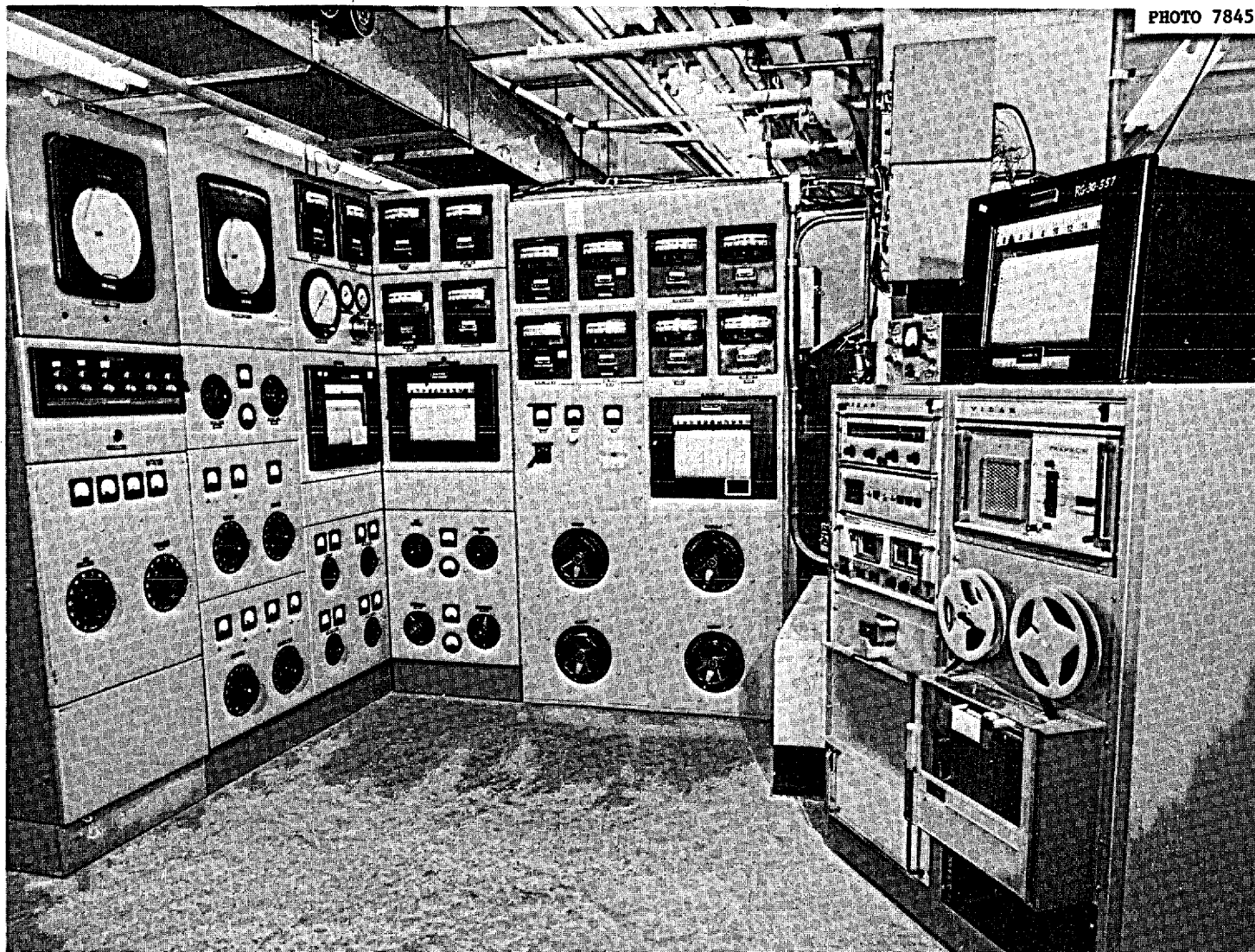


Fig. 7. Photograph of data recording equipment.

OPERATING PROCEDURES

In preparation for the addition of the molten salt mixtures, the system including the test section is heated to the desired temperature level above the melting point of the salt mixture. Approximately 165 lb of the molten salt is then introduced into one of the reservoirs by the force of argon gas pressure. Salt is forced back and forth through the test section as the operation of the apparatus is tested - for leaks, blockages, thermocouple and data recording functioning, etc. After the initial checkout procedure, the system is put on a standby mode by venting the gas pressure to the atmosphere and allowing the salt to siphon to equal levels in both reservoirs.* The standby mode is used to protect the test-section thermocouples by minimizing the heating of the test section.

Before each run, temperatures in the test section are raised to about 1000°F over a period of 45 minutes and the salt flow is reestablished. A fixed flow rate is established and power to the test-section heater is increased to the desired heat flux. When the temperatures indicate steady-state conditions, all parameters - power input, flow rate, and temperatures - are continuously recorded. The flow of salt is reversed when one reservoir is nearly empty, and the heat flux is momentarily reduced to about half the operating value to prevent a temperature excursion in the test section at the time of zero flow. The upper range of flow rates is limited by the time required to empty one of the reservoirs. Whenever the temperature exceeds the desired level, the system is allowed to cool by reducing the power to the test section and other appropriate heaters.

Periodic calibrations of radial heat losses were made by measuring the power required to maintain an empty test section in an isothermal condition as a function of temperature level. The information furnished by this calibration is used in each run, when an isothermal check of the test-section thermocouples is obtained at the desired temperature level

* This procedure resulted in several salt leaks when a number of power failures occurred during the standby condition. Melting of the confined salt was invariably accompanied by rupture of the thin-walled tubing due to the expansion of the salt upon partial melting. A better standby procedure would be to drain the salt into one reservoir, allowing unrestrained expansion of the salt during melting if an unexpected freeze should occur.

with the hot salt flowing and only enough heat added to the test section to equal the radial heat loss. In Fig. 8, typical test-section thermocouple readings from an isothermal run show a scatter band of $\pm 4^{\circ}\text{F}$ about the average outside wall temperature. The sheathed thermocouples in the mixing chambers read slightly higher during isothermal runs and are believed to be more accurate. Their readings, therefore, provide the basis for standardization and the tube wall readings are corrected to this standard.

Extensive tests were conducted to insure the reliability of the apparatus and experimental procedures. The first test-section tube produced erratic axial temperature patterns which did not improve with more thermal insulation of the test section. Subsequently, the anomalous axial temperature profiles were traced to the test section, in which a hole had burned through the wall and had been repaired by welding. Excessive weld material protruding into the tube was thought to have disturbed the temperature and velocity profiles. Replacement of the test section eliminated the difficulty.

Other possible sources of error were investigated during the search for the cause of the temperature irregularities. Electrical conduction through the molten salt would result in additional heating of the salt, but the ratio of the resistivity of the salt to that of the test section is greater than 2500, indicating very little heat generated in the salt in this manner. Additional calculations of the radial temperature distribution⁴ confirmed that not more than 0.2% of the power was expended by electrical conduction in the salt.

Temperature variations due to free convection are believed to be larger than those attributable to internal heating; but according to the criterion of Shannon and DePew,⁵ free convection in the horizontal test-section position is insignificant compared with forced convection in the range of Reynolds numbers described in this work.

As an additional check of natural-convection effects, the reactor fuel salt experiments were repeated with the test section anchored in a vertical position while other equipment arrangements and operational procedures remained unchanged. The object of the change was to compare the effects of free convection in the vertical and horizontal positions. A

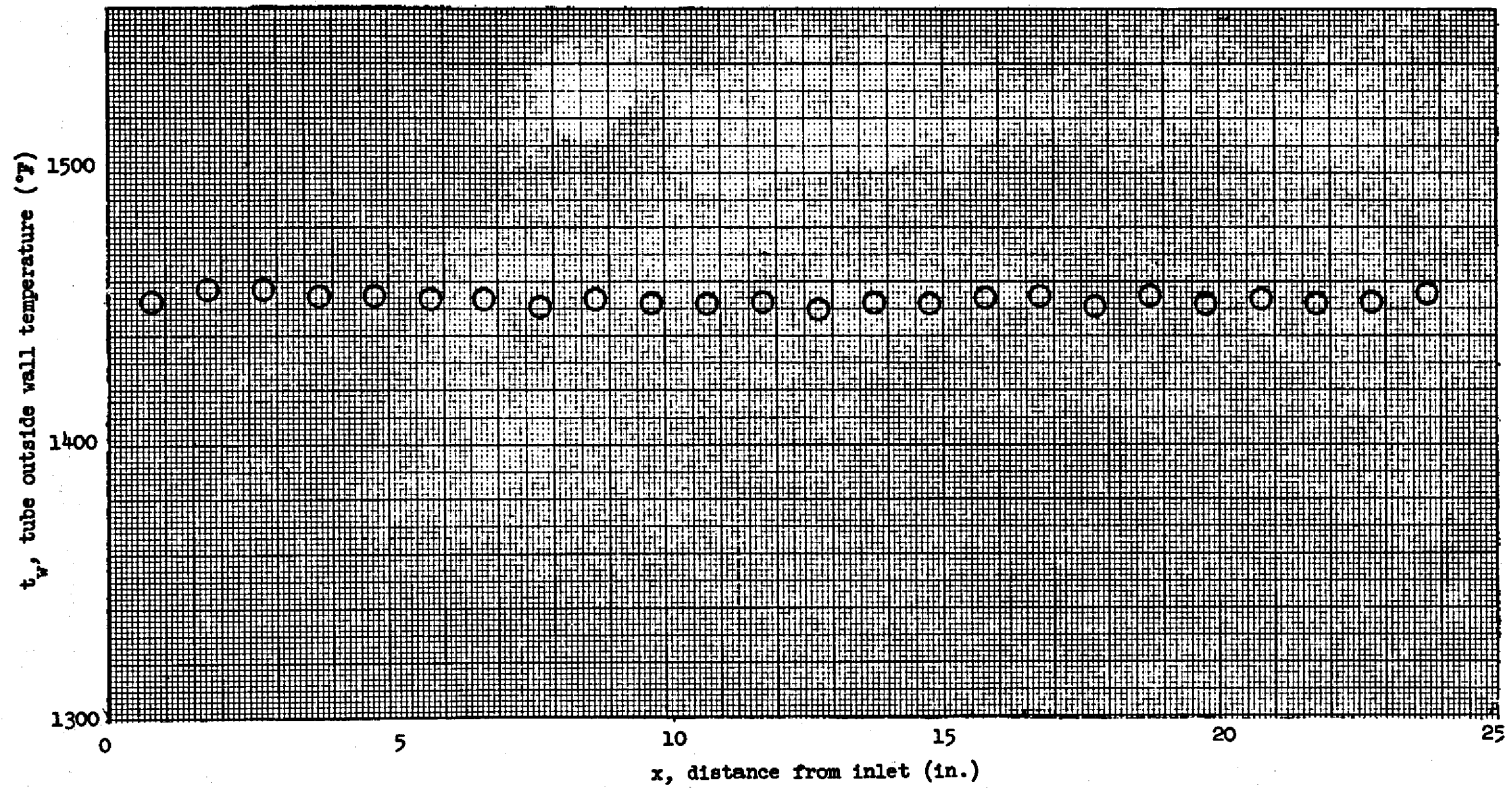


Fig. 8. Tube wall thermocouple readings during isothermal salt flow.

crack developed in one of the piping connections to the test section after 8 runs and repairs were not attempted. However, the results of the vertical runs did not show any difference in the effect of free convection as related to the orientation of the test section. The data are presented later in the report and in Appendix B.

The possibility of heat conduction losses to the electrodes at the ends of the test section prompted calculations to be made based on the conservative assumptions of maximum heat flux and a minimum Reynolds number. The results of these calculations show that the net heat conduction in the axial direction is less than 0.1% of the total heat generated in the test section at a distance of 0.25 in. from the entrance.

The electrical resistivity of the Hastelloy N test-section tube varies less than 1% in the temperature range of 1000 to 1500°F and the heat capacity of the salt varies less than 5% over the same temperature range. The variation of the radial heat loss along length of tube is less than 10% and the heat loss itself is less than 5%. A constant axial voltage drop measured along the test section verified the uniformity of the heat flux generated in the test-section wall and provided a check of the wall thickness and tube radius variation as a function of its length.

Experiments conducted with a well-known heat-transfer salt (HTS)* provided a final test in the new test section of the experimental procedure. Earlier experiments² showed that HTS data are well correlated by standard heat-transfer equations. The experiments with HTS in the present system demonstrated that the outside wall temperatures remained parallel to the mean salt temperature over half of the test-section length, indicating fully developed flow and a constant heat-transfer coefficient.

In 11 runs with HTS, the experimentally determined values of the heat-transfer coefficient were compared with those predicted by standard correlations. Ten of the values of the heat-transfer coefficient were within 13% of that predicted by the Sieder-Tate correlation⁶ and the other value was within 25%. Before the system was charged with reactor salts, the HTS was removed by extensively flushing with water and drying in heated vacuum for 10 days.

* HTS: KNO_3 - NaNO_2 - NaNO_3 (44-49-7 mole %).

CALCULATIONS

The local coefficient of forced-convective heat transfer is defined by the equation

$$h_x \equiv \frac{(q/A)_x}{(t_s - t_m)_x}, \quad (1)$$

where

h = coefficient of heat transfer, Btu/hr·ft²·°F; h_x , at position x along tube;

q = heat-transfer rate to fluid, Btu/hr;

A = heat-transfer (inner) surface area, ft²;

t = temperature, °F; t_m , fluid mixed mean at any position; t_s , inner surface of the tube at any position x ; t_w , outer surface of the tube at any position x .

Beyond the thermal and hydrodynamic entrance regions, h_x reaches an asymptotic value. For a constant heat flux, $(q/A)_x$, this limiting value will occur when $(t_s - t_m)_x$ reaches a constant value.

The inside tube wall temperature is related to the measured outside tube wall temperature by the equation

$$t_w - t_s = \frac{q + q_L}{2 \pi L k_m} \left[\frac{(r_w)^2}{(r_w)^2 - (r_s)^2} \ln \left(\frac{r_w}{r_s} \right) - \frac{1}{2} \right] - \frac{q_L}{2 \pi L k_m} \left(\ln \frac{r_w}{r_s} \right), \quad (2)$$

where

k = thermal conductivity of fluid, Btu/hr·ft·°F; k_m , thermal conductivity of tube;

L = test-section length, ft;

r = test-section tube radius, ft; r_s , inner surface; r_w , outer surface;

this is the solution to the one-dimensional steady-state heat conduction equation with a source term and a heat loss, q_L , at the outside wall.⁷ The only variable on the right-hand side of Eq. (2) is the thermal conductivity of the metal wall, k_m , which remains nearly constant over small temperature rises along the tube. Thus, when the temperature profiles t_w and t_m are parallel, the fluid flow in the tube is essentially fully developed.

For most of the measurements, the heat gained by the fluid in traversing the test section was calculated by the equation

$$q = wC_p(t_{m,o} - t_{m,i}) \quad (3)$$

in which

C_p = specific heat of fluid at constant pressure, Btu/lb·°F,

w = mass flow rate, lb/hr,

and subscripts

o = outlet

i = inlet.

For the later measurements (Runs 210 through 220), the heat gained by the fluid was determined from the electrical heat generation in the test section corrected for the calibrated heat loss. By calculating the heat input in this manner, the influence of the uncertainties in measuring the fluid mixed-mean inlet and outlet temperatures can be reduced.

The computer program used for reducing the experimental data is given in Appendix C.

RESULTS

Heat-transfer coefficients were determined experimentally in 70 runs covering the laminar, transition, and turbulent flow regimes. Ten runs with HTS to test the equipment are included with data shown in Appendix B. The physical properties and chemical analyses of the molten salt are listed in Appendix D, Tables D-1 and D-2, respectively.

The duration of a run usually permitted time for three thermocouple scans to demonstrate thermal steady state. Figure 9 shows typical outside wall temperatures and mean fluid temperatures. A straight line is drawn between the mean inlet and mean outlet fluid temperatures by assuming constant physical properties of the molten salt and uniform heat transfer over the inner surface of the test-section wall. These assumptions are supported by the constant heat capacity of the molten salt in the observed temperature range and the constant resistance of the Hastelloy N test section mentioned earlier.

ORNL-DWG 72-11517

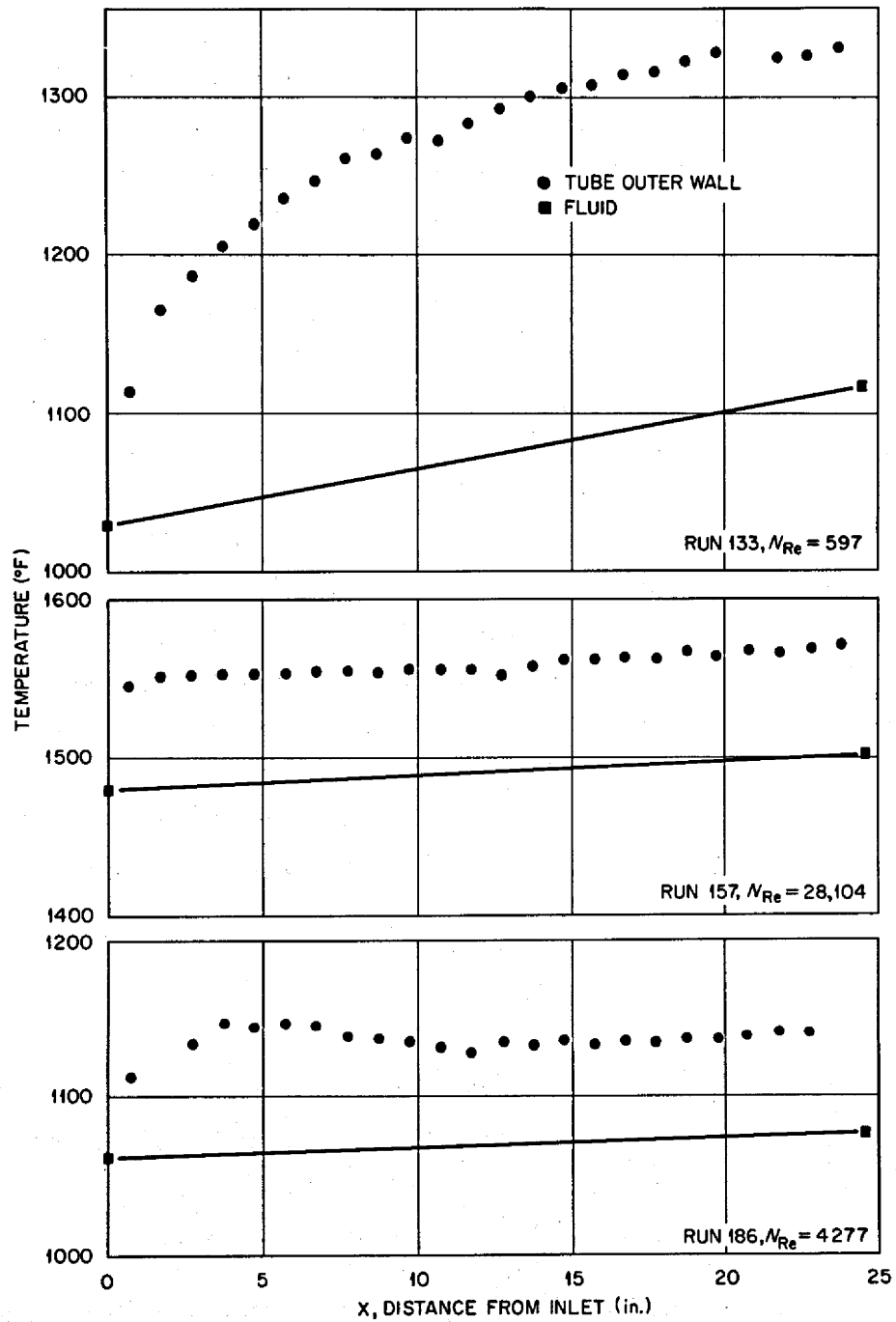


Fig. 9. Axial temperature profiles for molten salt flowing in a smooth tube at laminar ($N_{Re} = 597$), turbulent ($N_{Re} = 28,104$), and transition ($N_{Re} = 4277$) flow.

Three regions of N_{Re} are shown in Fig. 9 - the laminar, transition, and turbulent at $N_{Re} = 597, 4277, \text{ and } 28,104$, respectively. The coefficient of heat transfer h_x assumes its limiting value rapidly for turbulent flow; but in laminar and transition flows, a significant entrance region is evident. This entrance region is seen more clearly when h_x is plotted versus the distance along the test section x as in Fig. 10 for the transition flow run. After the thermal and hydrodynamic boundary layers become fully developed, h_x decreases to a limiting value. The test section is not long enough for h_x to reach the limiting value in laminar flow. Therefore, integrated values of h_x over the entire tube length, coupled with the parameter D/L , are used in developing the laminar flow correlations; whereas, the limiting constant h values are used for the transition and turbulent heat-transfer correlations.

Standard heat-transfer correlations for the three flow regimes are given in the following discussion of Eqs. (4) through (8). Heat-transfer data from the 70 runs are then presented in the dimensionless forms of standard correlations for comparison using the data listed in Appendix B and the physical properties in Table D-1.

1. For laminar, forced flow in the absence of natural convection, the equations of Sieder and Tate⁶ and Martinelli and Boelter⁸ are, respectively:

$$N_{Nu} = 1.86 [N_{Re} N_{Pr} (D/L)]^{1/3} (\mu/\mu_s)^{0.14} \quad (4)$$

and

$$N_{Nu} = 1.62 [N_{Re} N_{Pr} (D/L)]^{1/3} \quad (5)$$

2. For transition region flow beyond the entrance region, a modified form of Hausen equation² is:

$$N_{Nu} = 0.116 (N_{Re}^{2/3} - 125) N_{Pr}^{1/3} (\mu/\mu_s)^{0.14} \quad (6)$$

3. For turbulent flow, the equations recommended in Ref. 9 and attributed to McAdams and to Sieder and Tate are respectively:

$$N_{Nu} = 0.023 N_{Re}^{0.8} N_{Pr}^{0.4} \quad (7)$$

$$N_{Nu} = 0.027 N_{Re}^{0.8} N_{Pr}^{1/3} (\mu/\mu_s)^{0.14}$$

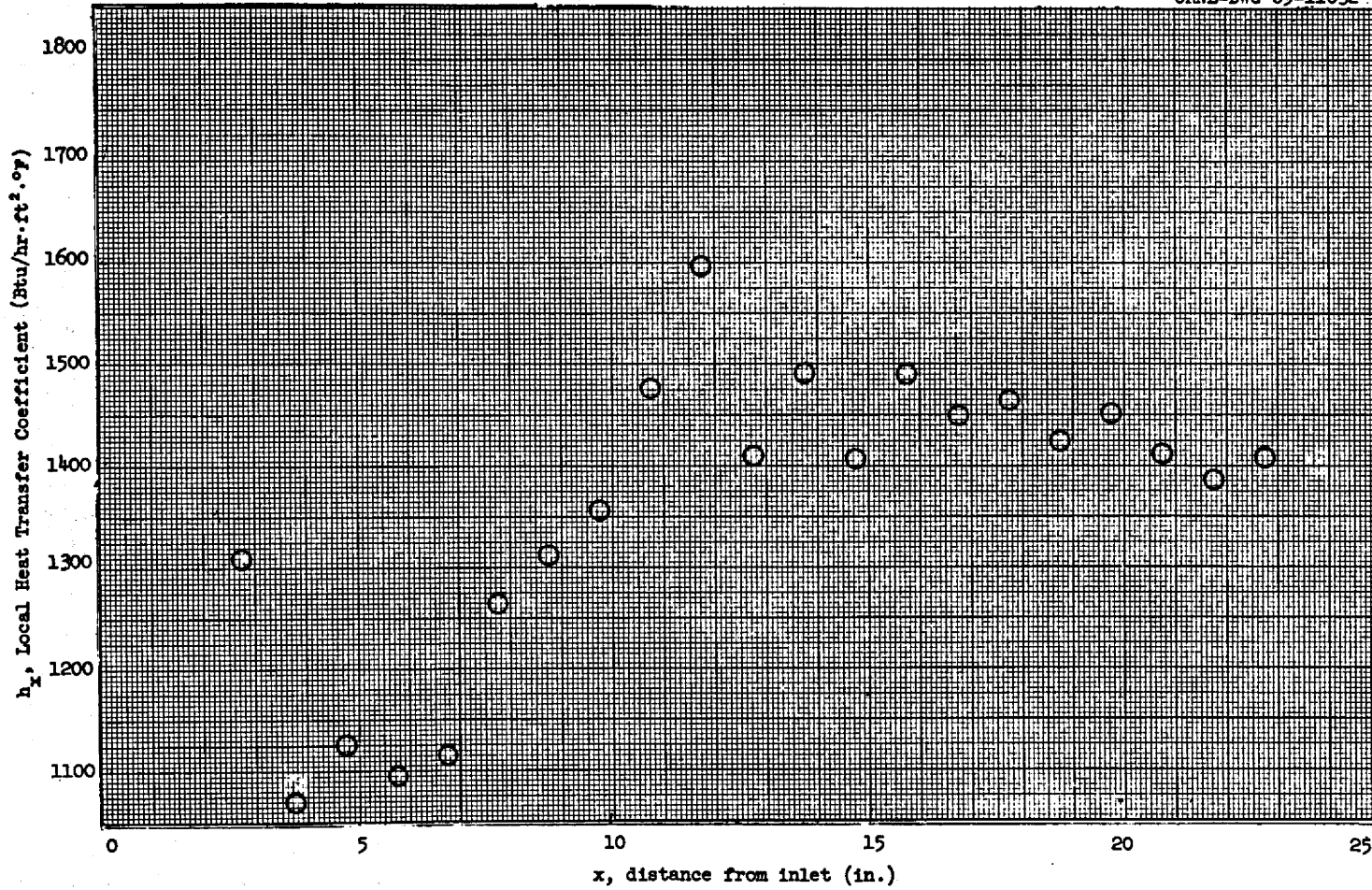


Fig. 10. Axial variation of the heat-transfer coefficient ($N_{Re} = 4277$).

where

$$\begin{aligned} N_{Nu} &= \text{Nusselt modulus, } hD/k, \text{ dimensionless,} \\ N_{Pr} &= \text{Prandtl modulus, } C_p \mu/k, \text{ dimensionless,} \\ N_{Re} &= \text{Reynolds modulus, } \rho V D/\mu, \text{ dimensionless,} \end{aligned}$$

and

$$\begin{aligned} V &= \text{mean velocity of fluid, ft/hr,} \\ D &= \text{inside diameter of tube, ft,} \\ \rho &= \text{fluid density evaluated at fluid mixed-mean temperature, lb/ft}^3, \\ \mu &= \text{fluid viscosity evaluated at fluid mixed-mean temperature,} \\ &\quad \text{lb/hr}\cdot\text{ft; } \mu_s, \text{ evaluated at temperature of the inner surface of} \\ &\quad \text{the tube.} \end{aligned}$$

Equations (4), (6), and (8) are compared with the experimental data in Fig. 11. The experimental results are in good agreement in the laminar region but are slightly below the equations representing the transition and turbulent regions. For example, in the range $3500 < N_{Re} < 30,000$, the data lie about 13% below Eqs. (6) and (8). The heat-transfer data could not be correlated in the transition range $2000 < N_{Re} < 4000$ because of entrance effects that persisted over the length of the test section. The laminar data do not fit Eq. (5) as well as Eq. (4), as shown by comparing Figs. 12 and 11. Similarly, Eq. (7) provides no significant improvement in the correlation of the data for $N_{Re} > 10,000$ over that of Eq. (8) [compare Figs. 13 and 11].

The data plotted in Figs. 11 through 13 suggest that the experimental data for laminar and turbulent flow can be fitted to functions of the form:

$$\text{Ordinate} = K N_{Re}^n, \quad (9)$$

where K and n are dimensionless constants having different values for laminar and turbulent flows and the "ordinate" is the ordinate used in Fig. 11. Least-squares fits of the data to the form of Eq. (9) were carried out assuming a constant value (1/3) for the Prandtl modulus exponent. These fits were tried with and without a viscosity ratio correction term. We found that when the viscosity ratio correction term was included, the values for the Reynolds modulus exponent, n , came closer to the commonly accepted values of 1/3 for laminar flow and 0.8 for turbulent flow. The resulting equations fitting the experimental

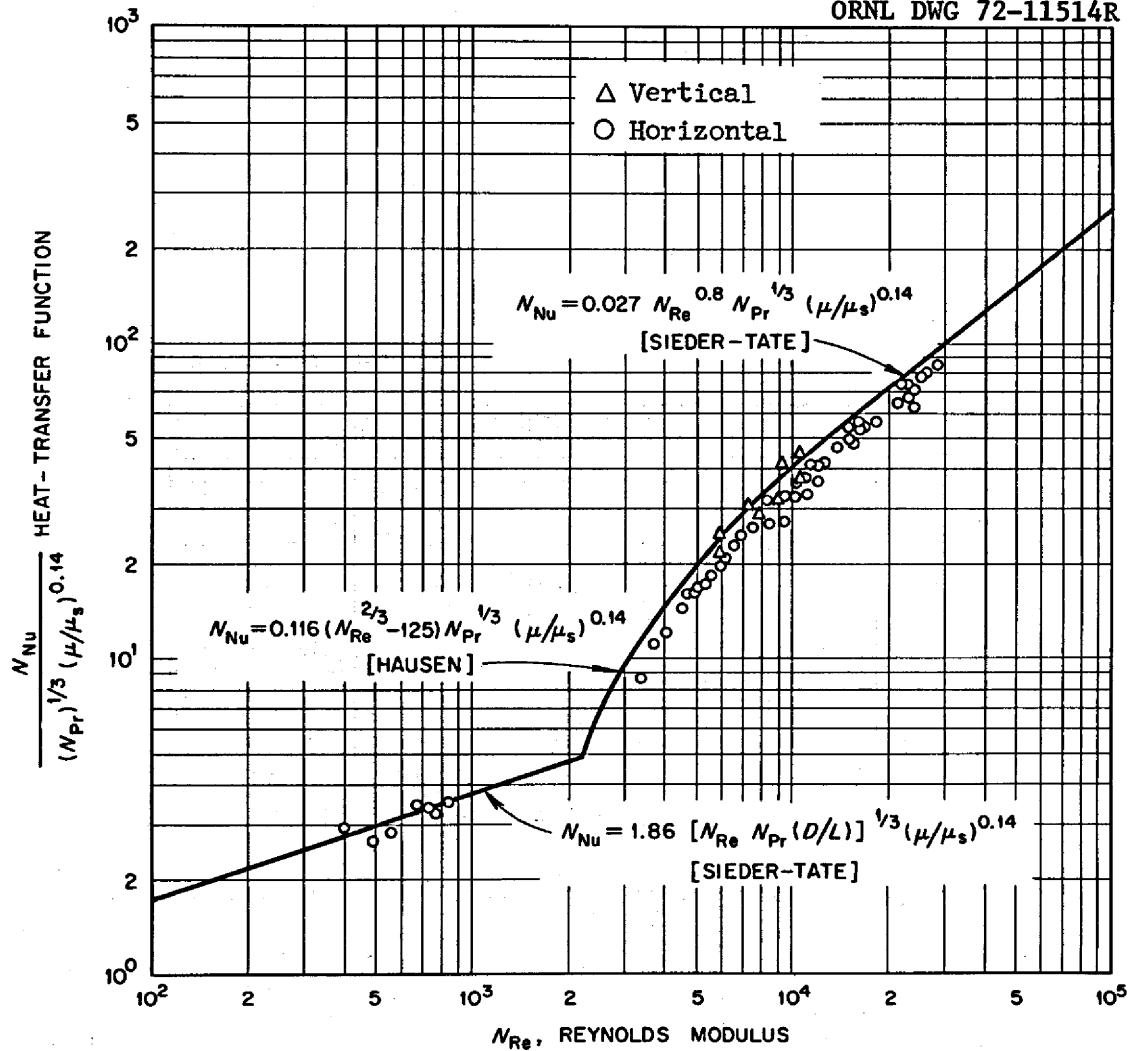


Fig. 11. Comparisons of the molten salt data for Eqs. (4), (6), and (8).

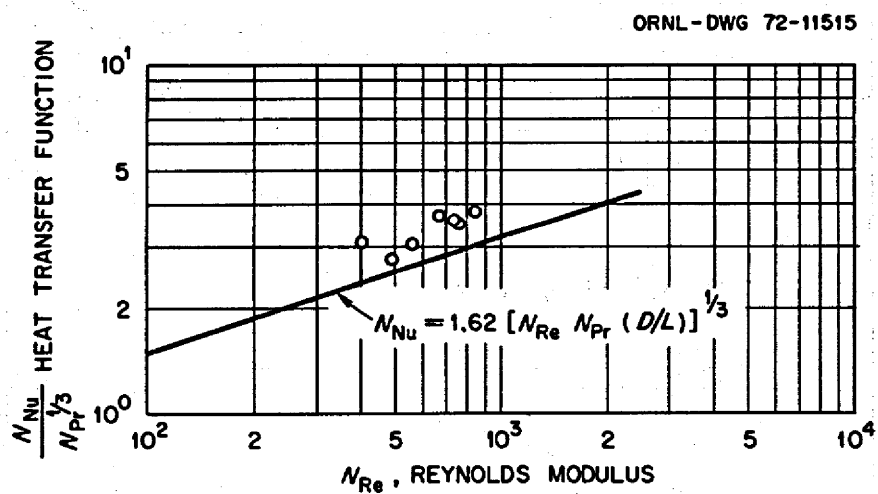


Fig. 12. Comparison of laminar flow data of molten salt with Eq. (5).

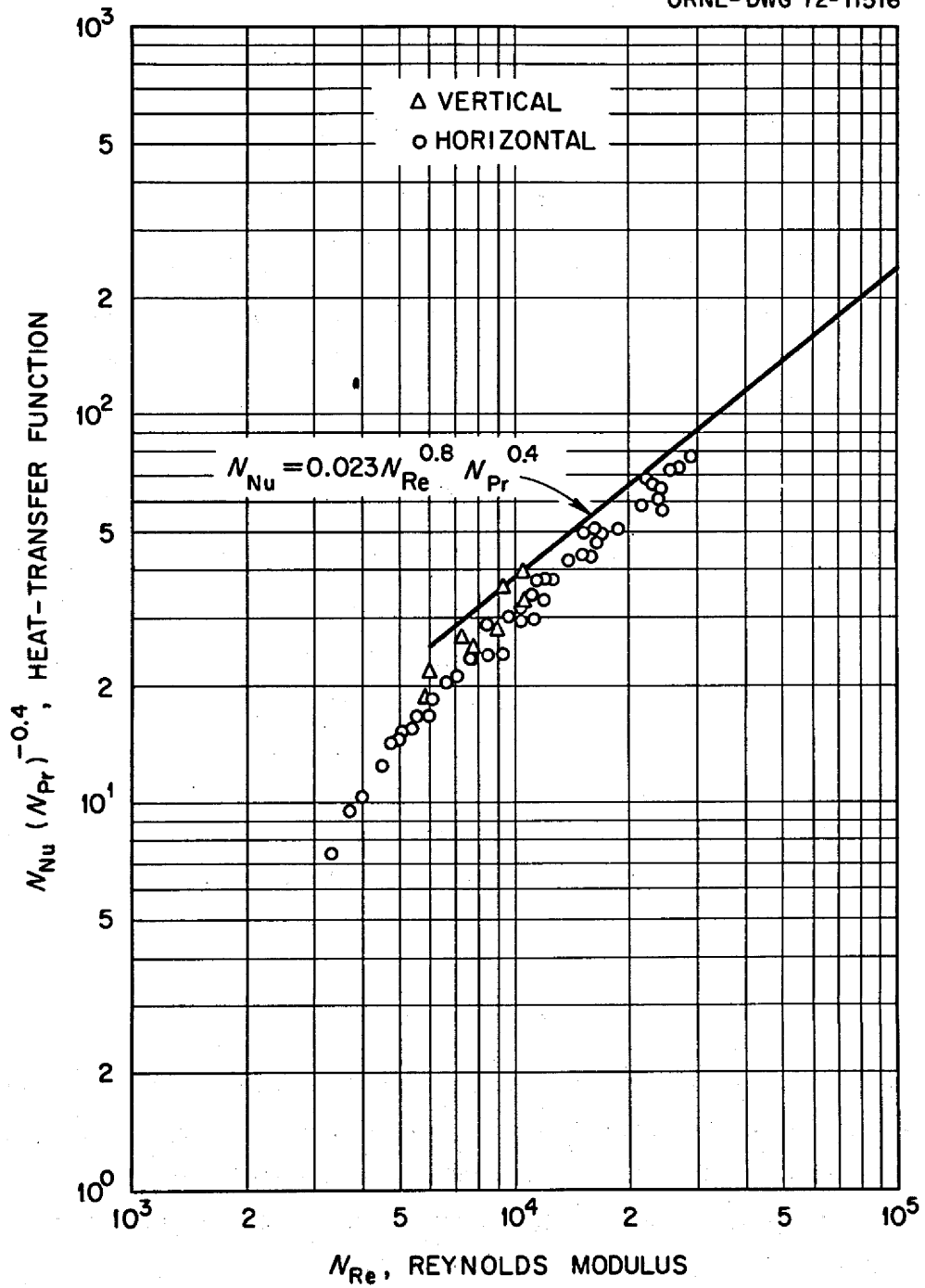


Fig. 13. Comparison of transition and turbulent data of molten salt with Eq. (7).

data are

$$N_{Nu} = 1.89 [N_{Re} N_{Pr} (D/L)]^{0.33} (\mu/\mu_s)^{0.14} , \quad (10)$$

with an average absolute deviation of 6.6% for $N_{Re} < 1000$; and

$$N_{Nu} = 0.0234 N_{Re}^{2/3} N_{Pr}^{1/3} (\mu/\mu_s)^{0.14} , \quad (11)$$

with an average absolute deviation of 6.2% for $N_{Re} > 12,000$.

Because the data in the transition region did not follow the form of Eq. (9), the equation for the experimental data in this range of N_{Re} was obtained by adjusting the coefficient in Eq. (6), giving the following relation:

$$N_{Nu} = 0.107 (N_{Re}^{1/3} - 135) N_{Pr} (\mu/\mu_s)^{0.14} , \quad (12)$$

with an average absolute deviation of 4.1% for $3500 < N_{Re} < 12,000$.

The heat-transfer measurements made with the test section oriented in a vertical position to test for the possible effects of free convection are in good agreement with the standard correlations, except for four higher points (see Figs. 11 and 13). These higher points were obtained with downflow in contradiction to the predicted enhancement of heat transfer with upflow. Thus, a systematic thermocouple error in one of the mixing chambers is the most probable cause of the higher results with downflow.

DISCUSSION

The results indicate that the proposed reactor fuel salt behaves as a normal fluid in the range $0.5 < N_{Pr} < 100$ with regard to heat transfer. It should be noted that uncertainties in the physical properties of the salts reflect as great an effect on the correlations as does the uncertainty in the heat-transfer coefficient.

Our data lie below the standard correlations in the turbulent and transition regions but not in the laminar region. If the deviations in our data were caused by low-conductance surface films or entrained gas, one would expect the effect to be apparent in all three regions. An uncertainty in the viscosity of the salt might explain the discrepancies in

the turbulent and the transition regions since the heat-transfer function in the laminar region is almost independent of the viscosity. In addition, the lower values in the transition regime could be the result of the failure of the thermal boundary layer to fully develop over the length of the test section.

The problem of boundary-layer development is most pronounced in the range of Reynolds number $2000 < N_{Re} < 4000$, where entrance effects persisted for the entire length of the test section. The same effect could be produced up to $N_{Re} = 5000$ at higher wall heat fluxes. Figure 14 illustrates the apparent effect of heat flux on the entrance region length. At $N_{Re} = 3762$ and a wall heat flux of 2.55×10^5 Btu/hr.ft², there is no region of constant heat-transfer coefficient. In contrast, temperature profiles at a similar Reynolds number, $N_{Re} = 3565$ and the lower wall heat flux of 0.74×10^5 Btu/hr.ft² show a constant heat-transfer coefficient over most of the test-section length. Since the viscosity of the fluid decreases with increasing temperature, heat transfer from the tube wall may be exerting a stabilizing effect on the laminar boundary layer,^{9,10} thus delaying transition.

Future experiments with the fuel salt should include system modifications so that the entrance region effects in transition flow can be better evaluated. Possible modifications would be the insertion of an unheated calming section prior to heat addition to permit establishment of the hydrodynamic boundary layer before changing the temperature profile. This would separate the two effects that now occur simultaneously. Another possibility would be to increase the length of the test section while maintaining a constant heat flux along the length. A sufficiently long tube might allow fully developed flow patterns to be reached before the test-section exit.

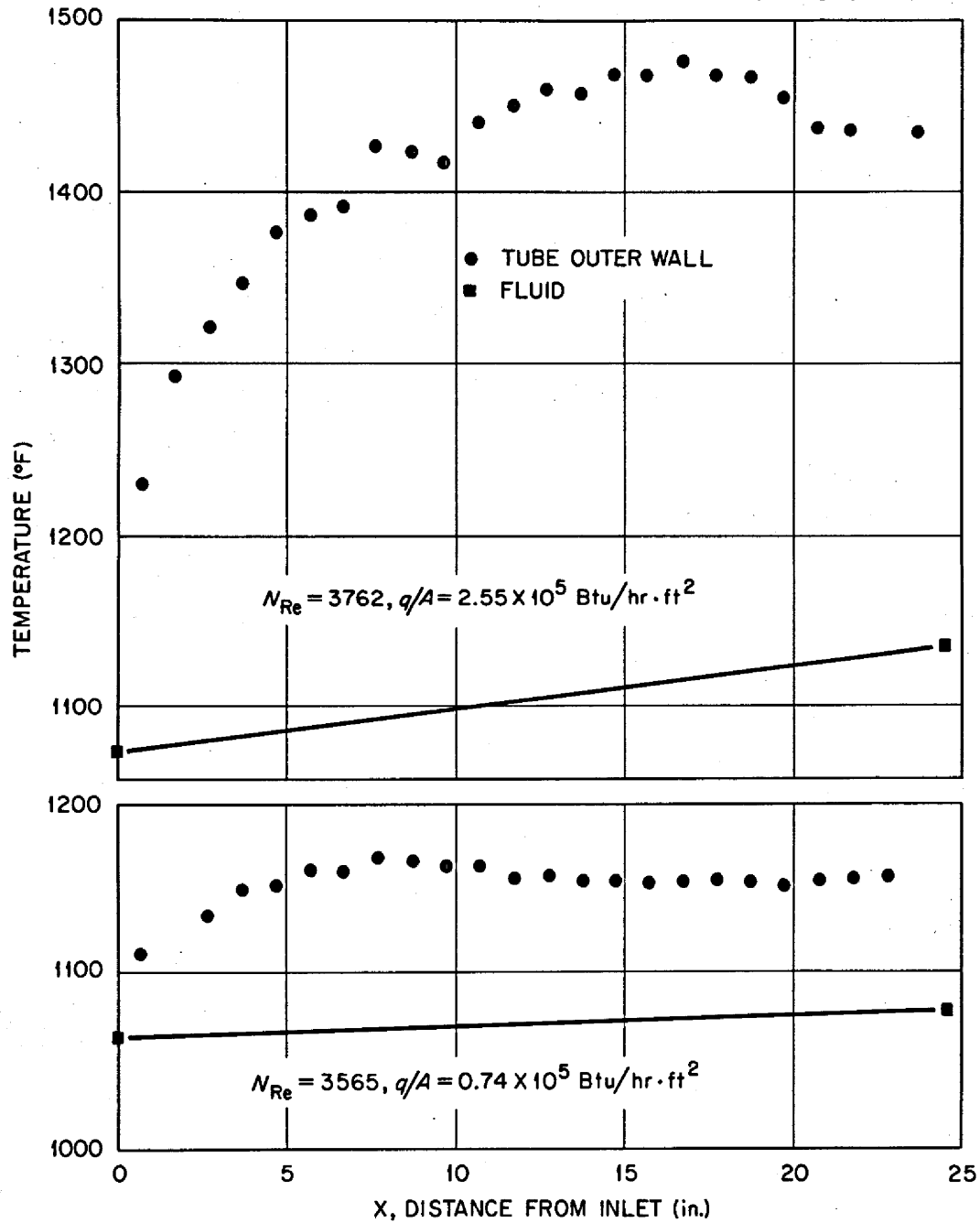


Fig. 14. Comparison of axial temperature profiles of the molten salt at similar N_{Re} with heat flux varied by a factor of 3.5.

CONCLUSIONS

We have found molten fluoride salt mixtures to behave, for the most part, as normal fluids with respect to forced-convection heating in a smooth tube. Although the present results average $\sim 13\%$ below the standard literature heat-transfer correlations, one must realize that some uncertainties exist in the physical properties of the salt and that the standard correlations themselves are based on heat-transfer data using fluids such as air, steam, water, petroleum, etc., which exhibit a $\pm 20\%$ scatter band around the standard curves.

No evidence of the existence or influence of low-conductance surface films, such as corrosion products, gases, or oxides, was found in the present studies. In the Reynolds modulus range from 2000 to 5000, we did find the heat-transfer coefficient to vary along the length of the tube in a manner which appeared related to a delay in the transition to turbulent flow. We believe this delay in transition is abetted by the stabilizing influence of heating a fluid whose viscosity has a large negative temperature coefficient. We intend to make further studies of this phenomenon.

ACKNOWLEDGMENTS

The design, construction, and operation of these experiments were made possible by the able assistance of J. J. Keyes, Jr., H. W. Hoffman, R. L. Miller, J. W. Krewson, W. A. Bird, and L. G. Alexander.

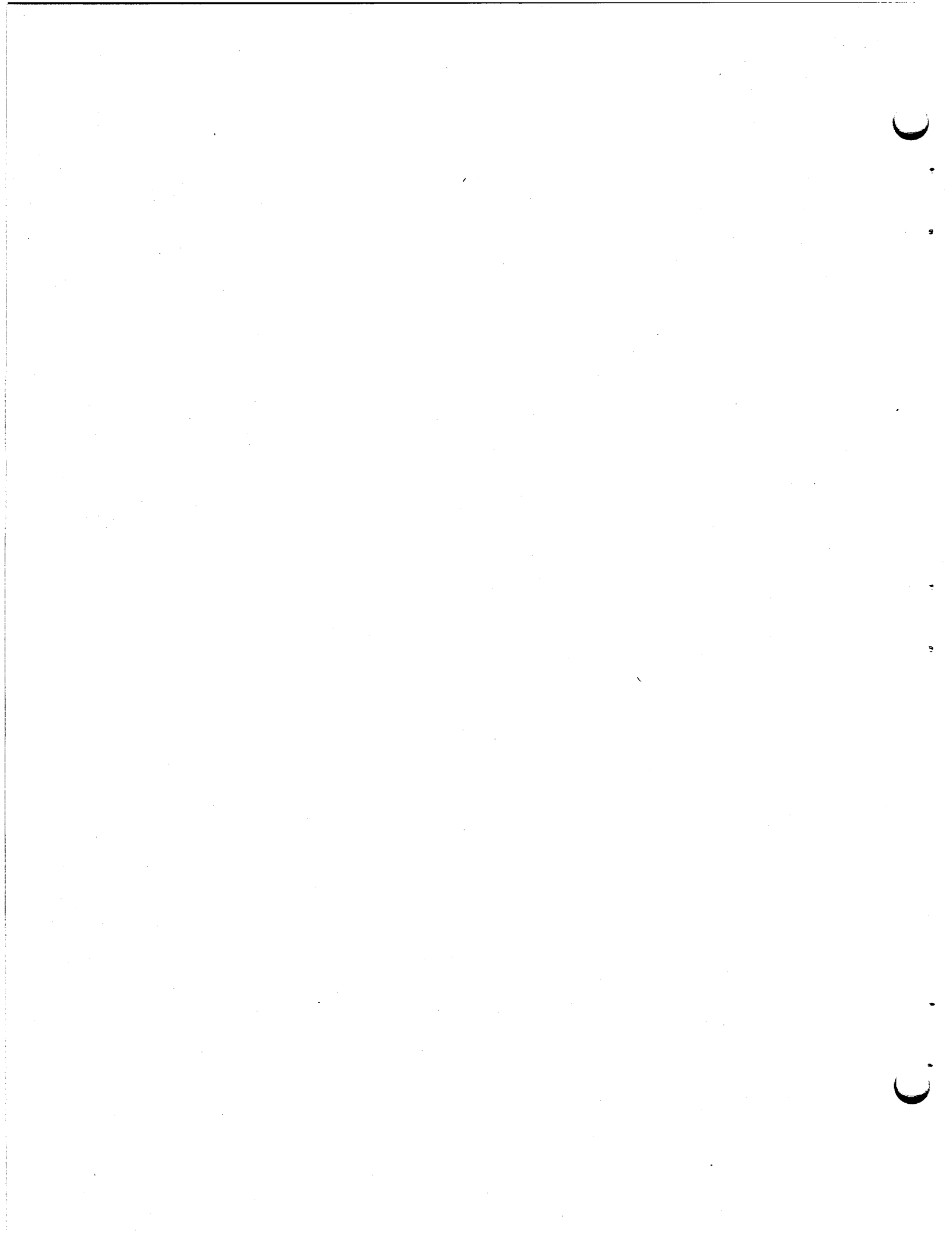
REFERENCES

1. H. W. Hoffman, Turbulent Forced-Convection Heat Transfer in Circular Tubes Containing Molten Sodium Hydroxide, USAEC Report ORNL-1370, Oak Ridge National Laboratory, October 1952; see also Proceedings of the 1953 Heat Transfer and Fluid Mechanics Institute, p. 83, Stanford University Press, Stanford, California, 1953.
2. H. W. Hoffman and S. I. Cohen, Fused Salt Heat Transfer - Part III: Forced-Convection Heat Transfer in Circular Tubes Containing the Salt Mixture $\text{NaNO}_2\text{-NaNO}_3\text{-KNO}_3$, USAEC Report ORNL-2433, Oak Ridge National Laboratory, March 1960.

3. H. W. Hoffman and J. Lones, Fused Salt Heat Transfer - Part II: Forced-Convection Heat Transfer in Circular Tubes Containing NaK-KF-LiF Eutectic, USAEC Report ORNL-1777, Oak Ridge National Laboratory, February 1955.
4. H. F. Poppendiek and L. D. Palmer, Application of Temperature Solutions for Forced-Convection Systems with Volume Heat Sources to General Convection Problems, USAEC Report ORNL-1933, Oak Ridge National Laboratory, September 1955.
5. R. L. Shannon and C. A. DePew, Forced Laminar Flow Convection in a Horizontal Tube with Variable Viscosity and Free-Convection Effects, ASME Technical Paper 68-WA/HT-20.
6. E. N. Sieder and G. E. Tate, Heat Transfer and Pressure Drops of Liquids in Tubes, Ind. Eng. Chem. 28(12): 1429-1435 (1936).
7. P. F. Massier, A Forced-Convection and Nuclear-Boiling Heat-Transfer Test Apparatus, JPL-TR-32-47, Jet Propulsion Laboratory, March 3, 1961.
8. E. R. G. Eckert, A. J. Diaguila, and A. N. Curren, Experiments on Mixed-Free-and-Forced-Convective Heat Transfer Connected with Turbulent Flow Through a Short Tube, NACA TN-2974, National Advisory Committee for Aeronautics, July 1953.
9. W. M. Rohsenow and H. Y. Choi, Heat, Mass, and Momentum Transfer, Prentice-Hall, Englewood Cliffs, New Jersey, 1961.
10. H. Schlichting, Boundary Layer Theory, 4th ed., McGraw-Hill, New York, 1960.
11. A. R. Wazzan, The Stability of Incompressible Flat Plate Laminar Boundary Layer in Water with Temperature Dependent Viscosity, pp. 184-202 in Proceedings of the Sixth Southeastern Seminar on Thermal Sciences, Raleigh, North Carolina, April 13-14, 1970.
12. S. Cantor, ed., Physical Properties of Molten-Salt Reactor Fuel, Coolant, and Flush Salts, USAEC Report ORNL-TM-2316, Oak Ridge National Laboratory, August 1968.
13. J. W. Cooke, Thermophysical Properties, pp. 89-93 in MSRE Semiann. Progr. Rept. Aug. 31, 1969, USAEC Report ORNL-4449, Oak Ridge National Laboratory.

APPENDIX A

ADDITIONAL DETAILS OF THE EXPERIMENTAL SYSTEM



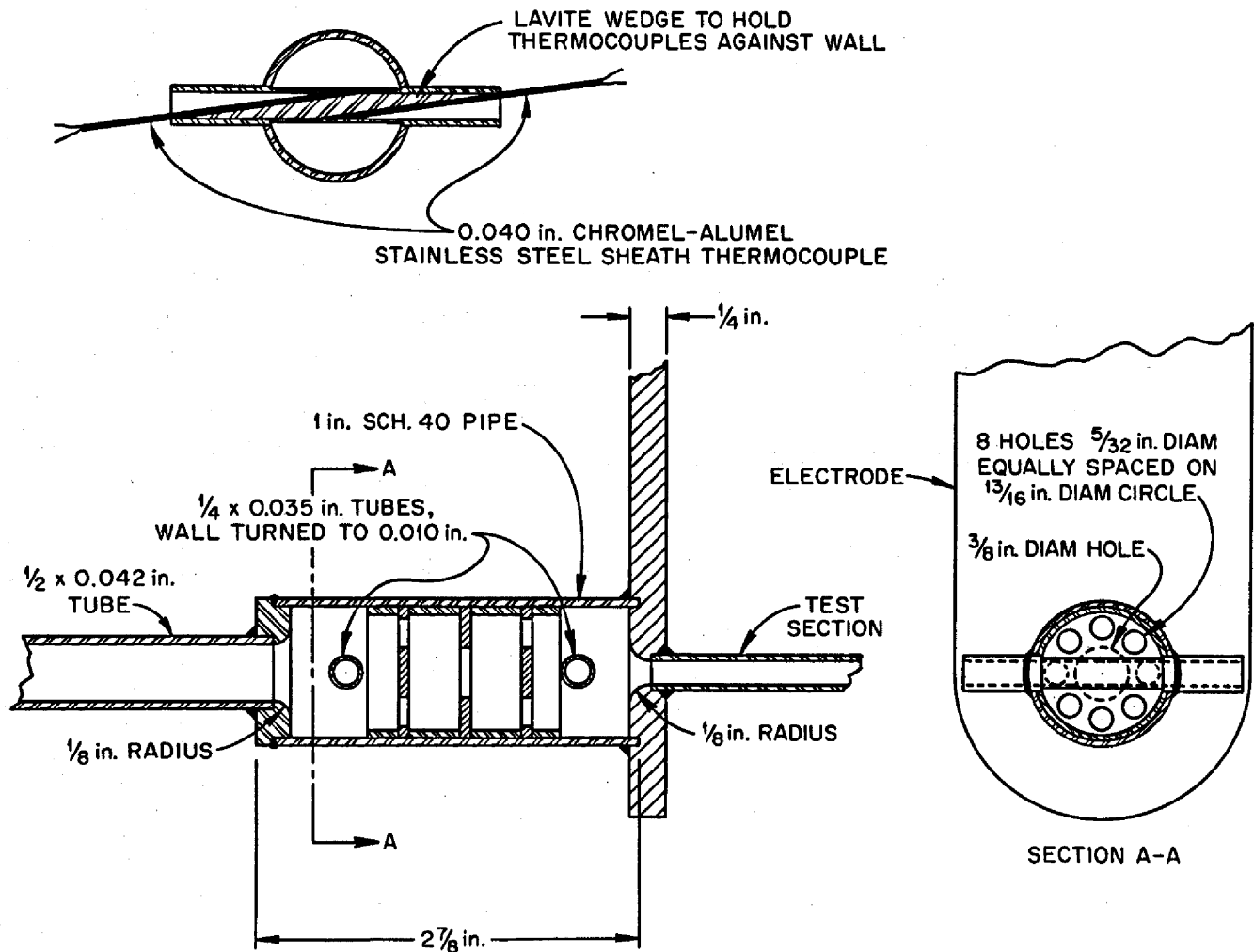


Fig. A-1. Mixing chamber weldment.

ORNL-DWG 72-11524

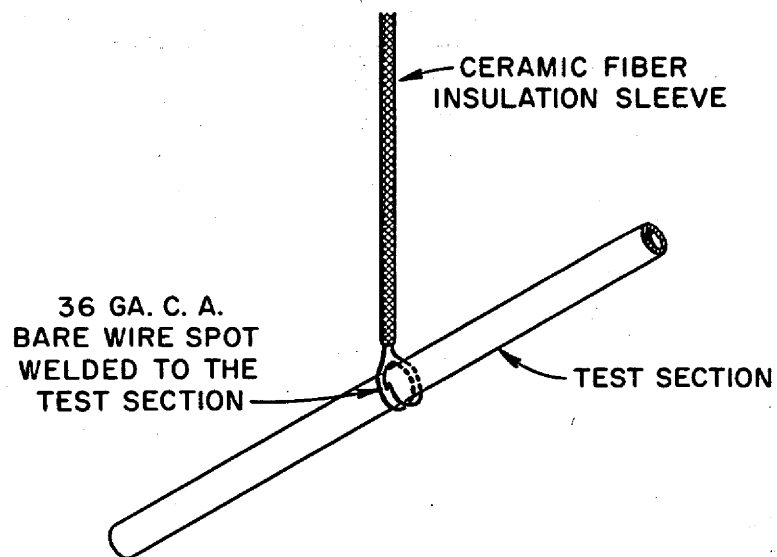


Fig. A-2. Scheme for the attachment of a test-section thermocouple.

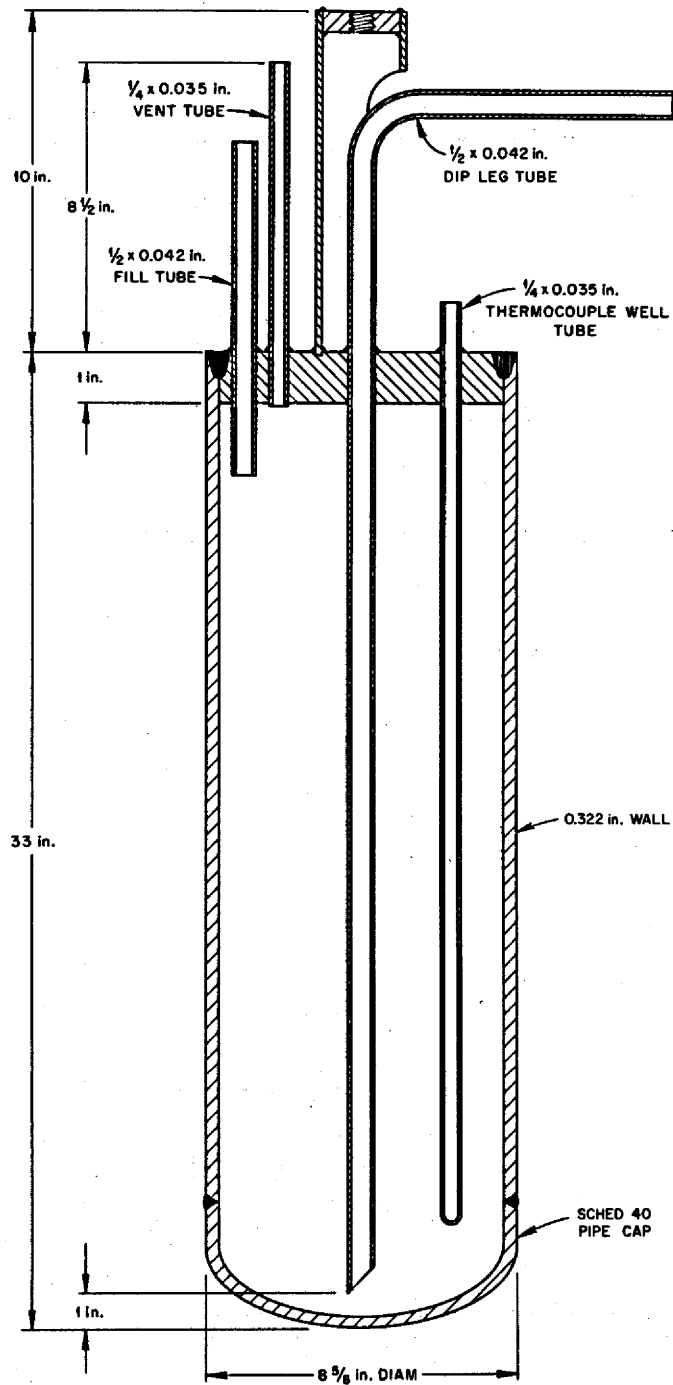


Fig. A-3. Detail of a Salt reservoir.

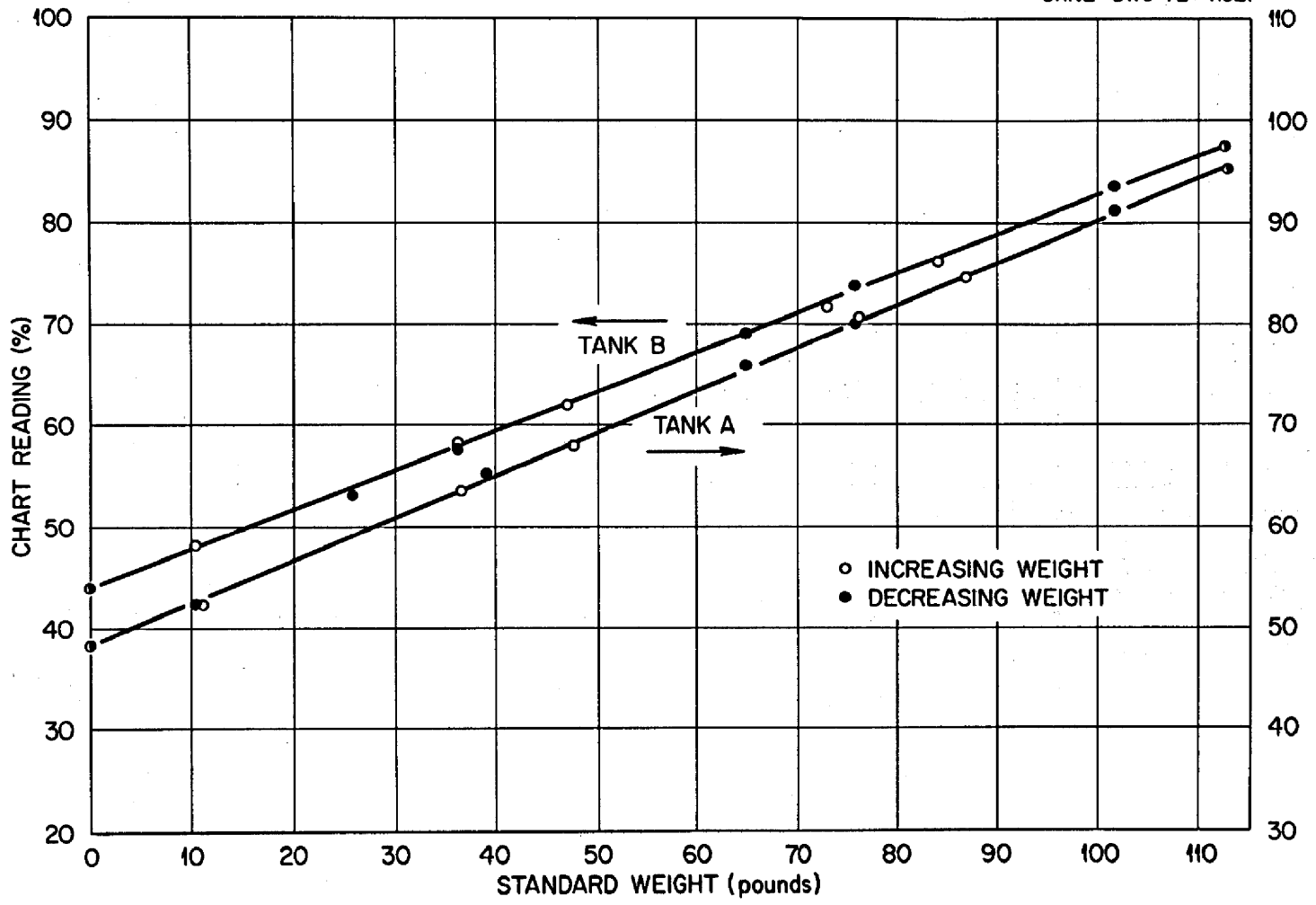


Fig. A-4. Weigh cell calibration curve.

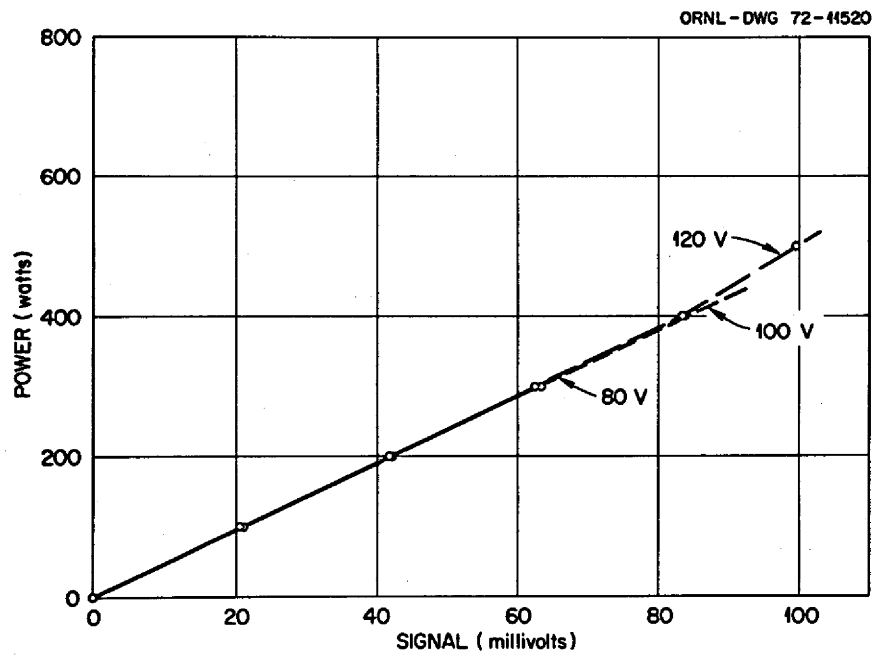


Fig. A-5. Wattmeter calibration curve.

PERTINENT EXPERIMENTAL EQUIPMENT

<u>Equipment</u>	<u>Capacity or Range</u>	<u>Accuracy</u>
<u>Load Cells</u> BLH electronics Type T3P1 and T3P2B	500 lb (150% overload) 3 mv/v input	±0.02% full scale (see Fig. A-4)
<u>Strip Recorder</u> Honeywell Model BY153X2VV-(W7) -(IV)A1 (modified)	L-2 Special	±0.25% full scale
<u>Current Transformer</u> Nothelfer windings Labs, Incorporated Model 14388	25 kva (prim. & sec.) 48 v prim. 4 x 250 amp sec	-
<u>Digital Voltmeter</u> Vidar Model 521	±10 mv to ±1000 v in 6 decade stages	±0.01% of full scale (least count 1.0 μv)
<u>System Coupler</u> Vidar Model 650-12	-	-
<u>Scanner</u> Cunningham Scannex Control Model 000113G	-	-
<u>Tape Digital Printer</u> Franklin Electronics, Inc.	-	-
<u>Tape Punch Process</u> Tally Corporation Model 1665 Tape Drive Model P150 Tape Reader Model 1848	-	-
<u>Wattmeter</u> General Electric Type 4701 Watt Transducer	2.5 - 10.0 in 2.5 steps	(see Fig. A-5)
<u>Thermocouple Reference- Junction Compensator</u> Universal Compensator Model RJ4801-CS	-	-
<u>Thermocouples</u> Chromel-Alumel	-	±0.75%

APPENDIX B
EXPERIMENTAL DATA

C

C

Table B-1. Experimental Data for Heat-Transfer Studies Using the
Salt LiF-BeF₂-ThF₄-UF₄; 67.5-20.0-12.0-0.5 mole %

Run No.	T _{in} (°F)	T _{out} (°F)	ΔT (°F)	w (lb/hr)	q/A (Btu/hr·ft ² × 10 ⁻⁵)	Heat Balance ^a	h (Btu/hr·ft ² ·°F)	\bar{N}_{Re}	\bar{N}_{Pr}	\bar{N}_{Nu}	N_{St}^b
107	1388.3	1436.0	47.7	2532.0	4.07	1.05	4882	15,993	6.3	106.1	56.000
115	1362.7	1415.8	53.1	1387.2	2.48	1.12	2831	8,345	6.6	61.5	31.902
117	1383.7	1438.4	54.7	1807.2	3.33	1.01	3617	11,419	6.3	78.6	41.497
119	1379.1	1436.6	57.5	1185.0	2.30	1.05	2302	7,495	6.3	50.0	26.270
121	1418.0	1474.4	56.4	2191.2	4.16	1.04	4590	14,917	5.8	99.8	54.082
122	1456.2	1507.9	51.7	2968.2	5.17	1.04	6192	21,647	5.5	134.6	74.415
123	1488.2	1537.8	49.6	3206.4	5.36	1.00	6462	25,119	5.1	140.4	79.762
127	1097.9	1156.4	58.5	1636.8	3.23	1.05	1936	5,005	13.1	42.1	16.713
129	1082.7	1163.3	80.6	250.8	0.68	1.01	396	738	13.5	8.6	3.359
130	1081.5	1177.1	95.6	279.6	0.90	1.00	427	839	13.3	9.2	3.563
131	1089.8	1159.9	70.1	227.4	0.54	1.02	407	673	13.5	8.8	3.488
132	1090.6	1160.2	69.6	256.2	0.60	0.97	381	760	13.4	8.3	3.265
133	1029.6	1118.7	89.1	221.4	0.66	0.93	357	550	15.9	7.7	2.821
134	1036.3	1134.8	98.5	155.4	0.52	0.93	358	405	15.3	7.8	2.944
143	1062.8	1117.7	54.9	1785.0	3.30	1.04	1940	4,940	14.5	42.2	16.148
144	1075.4	1135.7	60.3	1900.8	3.87	1.04	2200	5,523	13.8	47.8	18.563
145	1048.2	1103.4	55.2	2007.6	3.73	1.04	2129	5,304	15.0	46.3	17.459
146	1064.0	1115.9	51.9	2199.6	3.85	1.04	2513	6,026	14.6	54.7	20.984
147	1076.9	1131.0	54.1	2307.6	4.20	1.04	2727	6,573	14.0	59.2	23.072
148	1093.5	1148.3	54.8	2506.8	4.63	1.03	3068	7,583	13.2	66.7	26.549
149	1460.4	1482.9	22.5	1166.4	0.89	0.94	2230	8,393	5.6	48.5	27.007
150	1460.6	1489.5	28.9	1700.4	1.66	1.03	3434	12,260	5.5	74.7	41.743
151	1469.4	1488.4	19.0	2093.4	1.34	1.01	3977	15,282	5.5	86.4	48.472
152	1477.0	1501.8	24.8	2458.2	2.05	1.00	4573	18,300	5.4	99.5	56.022
153	1486.7	1513.4	26.7	2784.6	2.51	1.09	5426	21,235	5.6	117.9	65.520

Table B-1 (Continued)

Run No.	T _{in} (°F)	T _{out} (°F)	ΔT (°F)	w (lb/hr)	q/A (Btu/hr·ft ² × 10 ⁻⁵)	Heat Balance ^a	h (Btu/hr·ft ² ·°F)	\bar{N}_{Re}	\bar{N}_{Pr}	\bar{N}_{Nu}	\bar{N}_{St}^b
154	1496.1	1523.3	27.2	3057.0	2.80	1.04	5740	23,719	5.1	124.8	71.557
155	1466.3	1484.7	18.4	3205.2	1.99	1.02	5551	23,214	5.5	120.7	67.668
156	1475.0	1488.2	13.2	3262.2	1.45	0.99	5229	23,861	5.5	113.7	63.927
157	1479.7	1502.7	23.0	3505.8	2.72	1.07	6627	26,192	5.4	144.1	81.181
158	1466.3	1483.8	17.5	1282.2	0.76	0.89	2236	9,284	5.5	48.6	27.265
159	1466.7	1492.6	25.9	1401.6	1.22	0.99	2708	10,171	5.5	58.9	32.943
160	1471.3	1492.2	20.9	1512.0	1.06	0.93	2741	11,107	5.5	59.6	33.394
161	1472.4	1494.4	22.0	1615.2	1.20	0.99	3033	11,853	5.5	66.0	36.980
162	1463.7	1522.0	58.3	1254.6	2.46	1.04	2675	9,464	5.2	58.2	32.754
163	1470.0	1527.5	57.5	1425.6	2.76	1.05	3071	10,884	5.2	66.7	37.571
164	1480.0	1535.8	55.8	1513.8	2.85	1.07	3334	11,770	5.1	72.5	41.151
165	1486.9	1539.2	52.3	2105.4	3.71	1.02	4385	16,497	5.1	95.3	54.119
166	1501.6	1546.2	44.6	2803.2	4.21	1.06	5852	22,512	5.0	127.2	72.942
167	1513.9	1561.7	47.8	3471.0	5.60	1.02	6892	28,499	4.9	149.8	86.348
170	1064.6	1080.1	15.5	1797.0	0.94	0.97	1737	4,524	15.9	37.7	14.620
171	1066.3	1082.2	15.9	2346.0	1.26	1.01	2340	5,938	15.7	50.9	19.818
172	1069.8	1084.0	14.2	2722.8	1.31	1.05	2905	6,939	15.6	63.2	24.811
173	1049.0	1081.2	32.2	202.2	0.22	0.96	320	493	16.3	7.0	2.671
186	1061.6	1076.2	14.6	1597.8	0.79	0.94	1445	3,986	16.0	31.4	12.161
191	1062.0	1078.5	16.5	1318.2	0.74	0.94	1041	3,322	15.9	22.6	8.713
192	1064.6	1080.3	15.7	1460.4	0.77	0.99	1337	3,690	15.7	29.0	11.274
193	1235.2	1262.7	27.5	1106.4	1.03	1.01	1591	4,731	9.3	34.6	16.075
195	1247.0	1270.6	23.7	2333.4	1.86	1.04	3560	10,200	9.1	77.4	36.392
198	1255.8	1296.0	40.2	3001.8	4.07	1.04	4645	13,693	8.7	101.0	47.638
199	1273.2	1294.4	21.2	3219.6	2.30	1.09	4752	14,944	8.6	103.3	49.533

Table B-1 (Continued)

Run No.	T _{in} (°F)	T _{out} (°F)	ΔT (°F)	w (lb/hr)	q/A (Btu/hr·ft ² × 10 ⁻⁵)	Heat Balance ^a	h (Btu/hr·ft ² ·°F)	\bar{N}_{Re}	\bar{N}_{Pr}	\bar{N}_{Nu}	\bar{N}_{St}^b
200	1279.6	1303.7	24.1	3392.4	2.76	1.07	5050	16,088.0	8.4	109.8	53.017
201 ^c	1237.8	1263.8	26.0	1351.2	1.18	1.07	2406	5,892.4	9.14	52.3	24.7
202 ^c	1250.7	1272.6	21.9	1717.8	1.27	1.01	2762	7,660.9	8.94	60.0	28.6
203 ^c	1252.2	1276.2	24.0	2050.2	1.66	1.16	4029	9,200.0	8.89	87.6	41.9
204 ^c	1258.4	1282.4	24.0	2299.2	1.86	0.99	3625	10,435.5	8.79	78.8	37.7
205 ^c	1229.9	1255.0	25.0	1395.0	1.18	1.01	2119	5,910.9	9.41	46.1	21.5
206 ^c	1231.7	1255.4	23.7	1704.0	1.36	1.10	3004	7,238.9	9.39	65.3	30.7
207 ^c	1243.6	1268.1	24.5	2036.4	1.68	0.97	3122	8,947.4	9.08	67.9	32.1
208 ^c	1247.2	1270.6	23.4	2338.8	1.84	1.12	4337	10,359.7	9.00	94.2	44.9
210	1132.4	1156.1	70.1	2110	1.69	1.01	2416	6,512	12.5	52.5	22.15
211	1168.4	1215.4	150.8	2105	3.38	1.01	3049	7,696	10.8	66.3	28.96
212	1203.4	1226.7	59.9	2102	1.69	1.03	2823	8,230	10.2	61.4	27.89
213	1138.1	1168.7	30.6	2654	2.76	1.04	3477	8,566	12.2	75.6	32.07
214	1097.9	1149.6	51.7	2807	4.92	1.01	3573	8,297	13.3	77.7	31.27
215	1248.1	1256.1	8.0	2887	0.79	0.97	4335	12,374	9.2	94.2	44.98
216	1258.3	1276.2	18.0	2914	1.77	1.03	4490	12,957	8.8	97.6	46.89
217	1280.6	1310.6	30.1	2791	2.85	1.05	4616	13,454	8.2	100.3	49.10
218	1288.1	1341.7	53.6	2753	5.03	1.03	4915	14,035	7.7	106.9	52.56
219	1293.8	1383.2	89.4	1593	5.04	1.03	2999	8,620	7.3	65.2	32.12
220	1118.5	1155.7	136.1	1140	1.51	1.02	1082	3,554	12.8	23.5	9.60

^aHeat balance = (sensible heat gained by fluid + heat loss)/(electrical heat generation).

$$\bar{N}_{St} = \bar{N}_{Nu} (\bar{N}_{Pr})^{-1/3} (\mu/\mu_s)^{-0.14}$$

^cTest section oriented vertically.

Table B-2. Experimental Data for Heat-Transfer Studies Using the
Salt Hitec ($\text{KNO}_3\text{-NaNO}_2\text{-NaNO}_3$; 44-49-7 mole %)

Run No.	T_{in} (°F)	T_{out} (°F)	δT (°F)	w (lb/hr)	q/A (Btu/hr·ft ² × 10 ⁻⁵)	Heat Balance ^a	h (Btu/hr·ft ² ·°F)	\bar{N}_{Re}	\bar{N}_{Pr}	\bar{N}_{Nu}	\bar{N}_{St}^b
87	537.6	677.3	139.7	157.2	0.85	0.99	283.5	2,314	9.3	17.0	7.34
88	540.8	591.3	50.5	1375.2	2.69	1.05	2499.4	15,450	11.3	150.0	64.3
89	567.5	621.0	53.4	2071.8	4.30	0.98	3516.6	25,640	10.2	211.0	93.1
96	574.8	624.3	49.5	2195.4	4.21	1.08	4450.9	27,578	10.1	267.1	119.7
97	601.4	650.7	49.3	1589.4	3.04	1.00	3045.6	21,716	9.3	182.7	84.2
98	608.4	658.5	50.1	1097.4	2.13	1.06	2473.8	15,349	9.1	148.4	69.3
99	618.5	672.5	54.0	630.6	1.32	1.03	1386.4	9,165	8.7	83.2	39.2
101	608.8	702.4	93.6	592.8	2.15	1.10	1332.4	9,065	8.3	79.9	37.6
102	633.1	657.2	24.1	640.2	0.60	0.99	1656.8	9,142	8.9	99.4	47.7
103	618.8	634.8	16.1	1551.6	0.97	1.05	4151.9	20,848	9.4	249.1	117.6
104	582.2	669.1	86.9	1603.8	5.41	0.99	3096.6	22,357	9.1	185.8	84.1

^aHeat balance = (sensible heat gained by fluid + heat loss)/(electrical heat generation).

$$\bar{N}_{St}^b = \bar{N}_{Nu} (\bar{N}_{Pr})^{-1/3} (\mu/\mu_B)^{-0.14}$$

APPENDIX C
COMPUTER PROGRAM

C

C

```

COMPILER OPTIONS - NAME= MAIN,OPT=02,LINECNT=6,SOURCE,EBCDIC,NOLIST,DECK,LOAD,MAP,NOEDIT,NCID,NOXREF
C I AM A MOLTEN SALT HEAT TRANSFER PROGRAM
ISN 0002 REAL L,MDOT,K1,K2,K3,K4,AUNC,MU,NJAVG,NGC,KINOW 10
ISN 0003 DIMENSION TO(30),XL(30),TI(30),TB(30),H(30),IN(200),OU(200),D(200) 12
ISN 0004 DIMENSION NUNO(30) 13
ISN 0005 INTEGER CTC 15
ISN 0006 6 DO 10 J=1,13 30
ISN 0007 IL=5*(J-1)+1 40
ISN 0008 IU=5*J 50
ISN 0009 READ 7,(IN(I),DU(I),I=IL,IU) 60
ISN 0010 7 FORMAT(5(I3,F5.2,2X)) 70
ISN 0011 10 CONTINUE 75
ISN 0012 DO 20 I=1,IU 76
ISN 0013 I1=IN(I)+1 77
ISN 0014 IF(DU(I).GE.0.01) D(I1)=DU(I) 77A1
ISN 0016 20 CONTINUE 77A2
ISN 0017 IF(D(45).LT.900.) GO TO 21 77B
ISN 0019 GO TO 22 77C
ISN 0020 21 D(46)=-D(46) 77D
ISN 0021 22 CONTINUE 77E
ISN 0022 DO 30 I=1,50 78A
ISN 0023 DU(I)=D(I) 78B
ISN 0024 30 CONTINUE 78C
C TEMP FIT FOLLOWS FOR 150 F REF JUNCTION W/F TO 1900 DEGREES F 79
ISN 0025 DO 420 I=1,46 79A
ISN 0026 IF(D(I).LT.1.59) GO TO 400 79B
ISN 0028 IF(D(I).GE.1.99.AND.D(I).LT.5.30) GO TO 401 79C
ISN 0030 IF(D(I).GE.5.01.AND.D(I).LT.10.01) GO TO 402 79D
ISN 0032 IF(D(I).GE.10.01.AND.D(I).LT.13.01) GO TO 403 79E
ISN 0034 IF(D(I).GE.13.01.AND.D(I).LT.17.01) GO TO 404 79F
ISN 0036 IF(D(I).GE.17.01.AND.D(I).LT.22.99) GO TO 405 79G
ISN 0038 IF(D(I).GE.22.99.AND.D(I).LT.29.99) GO TO 406 79H
ISN 0040 IF(D(I).GE.29.99.AND.D(I).LT.33.00) GO TO 407 79I
ISN 0042 IF(D(I).GE.33.0.AND.D(I).LT.36.0) GO TO 408 79J
ISN 0044 IF(D(I).GE.36.0.AND.D(I).LT.39.0) GO TO 409 79K
ISN 0046 IF(D(I).GE.39.0) GO TO 410 79L
ISN 0048 400 D(I)=150.+(236.-150.)/1.99*(D(I)-0.) 79L1
ISN 0049 GO TO 420 79M
ISN 0050 401 D(I)=236.+(371.-236.)/(5.01-1.99)*(D(I)-1.99) 79N
ISN 0051 IF(D(I).GE.258. .AND.D(I).LE.290.) D(I)=D(I)-0.6 79N1
ISN 0053 IF(D(I).GE.280. .AND.D(I).LE.314.) D(I)=D(I)-0.5 79N2
ISN 0055 GO TO 420 79O
ISN 0056 402 D(I)=371.+(592.-371.)/(10.01-5.01)*(D(I)-5.01) 79P
ISN 0057 IF(D(I).GE.532.00) D(I)=D(I)-0.80 79P1
ISN 0059 D(I)=D(I)+1.0 79P2
ISN 0060 IF(D(I).LE.425.) C(I)=D(I)-0.20 79P3
ISN 0062 GO TO 420 79Q
ISN 0063 403 D(I)=552.+(721.-592.)/(13.01-10.01)*(D(I)-10.01) 79R
ISN 0064 GO TO 420 79S
ISN 0065 404 D(I)=721.+(891.-721.)/(17.01-13.01)*(D(I)-13.01) 79T
ISN 0066 GO TO 420 79U
ISN 0067 405 D(I)=891.+(1143.-891.)/(22.99-17.01)*(D(I)-17.01) 79V
ISN 0068 GO TO 420 79W
ISN 0069 406 D(I)=1143.+(1444.-1143.)/(30.00-22.99)*(D(I)-23.00) -0.10 79X
ISN 0070 IF(D(I).GE.1396.) D(I)=D(I)+.3 79X1
ISN 0072 IF(D(I).LE.1234.) C(I)=D(I)+.30 79X2
ISN 0074 GO TO 420 79Y
ISN 0075 407 D(I)=1444.+(1576.-1444.)/(33.00-29.99)*(D(I)-29.99) 79Z
ISN 0076 IF(D(I).LE.1528.) D(I)=D(I)-0.5 79Z1

```

ISN 0078		GO TO 420	79AA
ISN 0079	408	D(I)=1576.+(1710.-1576.)/(36.00-33.00)*(D(I)-33.00)	79BB
ISN 0080		IF (D(I).GE.1635..AND.D(I).LE.1670.) D(I)=D(I)+0.4	79BB0
ISN 0082		GO TO 420	79BB1
ISN 0083	409	D(I)=1710.+(1848.-1710.)/(39.00-36.00)*(D(I)-36.00)+.10	79CC
ISN 0084		GO TO 420	79CC1
ISN 0085	410	D(I)=1648.+(1941.-1848.)/(41.00-39.00)*(D(I)-39.00) -.10	79CC2
ISN 0086		IF (D(I).GE.1892.) D(I)=D(I)+0.5	79CC3
ISN 0088	420	CONTINUE	79DD
ISN 0089		PRINT 23	80
ISN 0090	23	FORMAT(1H1)	80A
ISN 0091		DO 25 I=1,20	80A1
ISN 0092		J=D(50)+.2	80B
ISN 0093		PRINT 24,J	80C
ISN 0094	24	FORMAT(1HO,'NEXT IS RUN ',I4)	80D
ISN 0095	25	CONTINUE	80E
ISN 0096		D(41)=DU(41)	81A
ISN 0097		D(42)=DU(42)	81A
ISN 0098		FTC=DU(41)+0.2	100
ISN 0099		CTC=DU(42)+0.2	101
ISN 0100		UWAVG=AVG(C,1,24,.,750,23,750)	110
ISN 0101		CALL TKER(C,46,UWAVG)	120
ISN 0102		PRINT 51	132
ISN 0103	51	FORMAT (1H1,4X,9H SUBSCRIPT,6X,6HU CAT,9X,6HC DATA)	133
ISN 0104		DO 58 I=1,50	134
ISN 0105		PRINT 52,I,DU(I),C(I)	135
ISN 0106	52	FORMAT(7X,I3,8X,F8.2,8X,F8.2)	136
ISN 0107	58	CONTINUE	137
		C CONSTANTS FOLLOW. THE THERMAL K'S ARE TEMP DEPENDENT	139
ISN 0108		R1=-.180/2.	140
ISN 0109		D1=0.180/12.	141
ISN 0110		R2=-.250/2.	150
ISN 0111		R3=6.00/2.	160
ISN 0112		R4=3.0598	170
	C	K1 IS GIVEN ON CARD 845	180
ISN 0113		K2=0.06	190
ISN 0114		K3=9.00	200
ISN 0115		K4=14.32	210
ISN 0116		N=2	220
ISN 0117		L=24.5	230
ISN 0118		SPH1=0.324	236
ISN 0119		DXA=0.5	240
ISN 0120		DXB=0.5	250
		C END OF CONSTANTS	255
ISN 0121		XL(1)=.750	260
ISN 0122		DX=1.00	270
ISN 0123		DO 60 I=2,24	280
ISN 0124		M=I-1	285
ISN 0125		XL(I)=XL(M)+DX	290
ISN 0126	60	CONTINUE	300
ISN 0127		TAO=(D(27)+D(28))/2.	305
ISN 0128		TAI=(D(29)+D(30))/2.	310
ISN 0129		TBB1=(D(31)+D(32))/2.	315
ISN 0130		TBB0=(D(33)+D(34))/2.	320
ISN 0131		IF(TAO.GT.TAI)GO TO 61	325
ISN 0133		TA=TAI	330
ISN 0134		GJ TO 62	335
ISN 0135	61	TA=TAO	340

ISN 0136	62	IF (T880.GT.T881) GO TO 63	345
ISN 0138		T88=T881	350
ISN 0139		G) TO 64	355
ISN 0140	63	T88=T880	360
ISN 0141	64	CONTINUE	365
ISN 0142		IF (TA-T88)66,68,68	390
ISN 0143	66	TIN=TA	400
ISN 0144		TOUT=T88	410
ISN 0145		GO TO 70	420
ISN 0146	68	TIN=TB8	430
ISN 0147		TOUT=TA	440
ISN 0148	70	CONTINUE	450
ISN 0149		IF (TA-T88) 73,71,71	460
ISN 0150	71	DO 72 I=1,24	470
ISN 0151		M=25-I	475
ISN 0152		TO(I)=C(M)	480
ISN 0153	72	CONTINUE	490
ISN 0154		GO TO 80	500
ISN 0155	73	DO 75 I=1,24	510
ISN 0156		TO(I)=C(I)	520
ISN 0157	75	CONTINUE	530
ISN 0158	80	CONTINUE	540
		C CARE MUST BE TAKEN WITH REGARD TO SIGN CONVENTION FOR FOLLOWING Q AND DT	550
ISN 0159		QWM=400./83.6*D(47)*200.*3.412/D(49)	560
ISN 0160		MDOT=D(48)*60.	570
ISN 0161		DT=UWAVG - D(46)	575
ISN 0162		QLCAL=-(40.2757E-3)*CT*DT + 0.1100*DT - 0.1724E-11	576
ISN 0163		QLF=QLCAL/(2.*3.14*R2*L/144.)	577
ISN 0164		QLF=-QLF	578
ISN 0165		QEL=K4*.375*17./8./12.*(D(43)-D(25))/DXA+(D(44)-D(26))/DXB)	580
ISN 0166		DT=AVG(D,1,24.,750,23.750) - D(46)	585
ISN 0167		QINS=2.*3.14*(L-0.5)/12.*(-DT)/(ALOG(R3/R2)/K2+ALOG(R4/R3)/K3)	590
ISN 0168		QLEST=QEL + QINS	610
ISN 0169		QF=MDOT*SPH1*(TOUT-TIN)	640
ISN 0170		QODP= QF / (2.*3.14*R1*L)*144.	650
ISN 0171		QBAL=(QF-QLCAL)/QWM	660
ISN 0172		X1=FTC	710
ISN 0173		X1=X1-.250	720
ISN 0174		X2=FTC+CTC-1	730
ISN 0175		X2=X2-.250	740
ISN 0176	110	PRINT 111	810
ISN 0177	111	FORMAT (1H1,09X,1HX,11X,3HX/D,10X,1MH,11X,2MT6,11X,2MT1,11X,2HTO,12X,2HNU,11X,2HRE,12X,2HPR)	820
	8		821
ISN 0178	DO 115	I=1,24	830
ISN 0179		X=XL(I)	840
ISN 0180		ATT=TO(I) - 25.	841
ISN 0181	112	K1=TK(ATT)	845
ISN 0182		TI(I)=TC(I)-(QF - QLCAL) / (2.*3.14*L/12.*K1)* (R2*R2/(R2*R2-R1*R1)*ALOG(R2/R1)-0.500) +QLF*R2/12./K1*ALOG(R2/R1)	850 851 852
	8		862
ISN 0183		ATT=(TI(I)+TO(I))/2.	863
ISN 0184		K1NOW=TK(ATT)	864
ISN 0185		DK=ABS(K1NOW-K1)	865
ISN 0186		IF (DK.GE.0.1) GO TC 112	870
ISN 0188		XOD=X/(2.*R1)	880
ISN 0189		TB(I)=TIN + QODP*3.14*2.*R1*X/MDCT/SPH1/144.	890
ISN 0190		HI(I)=QODP/(TI(I)-TB(I))	895
ISN 0191		CALL PRCP(IREO,PRNC,PU,RHO,TB(I),R1,CCND,SPH1,MDOT)	

ISN 0192		NUNO(I)=H(I)*2.*R1/12./CCND	897
ISN 0193		PRINT 114,X,XOD,H(I),TB(I),TI(I),TO(I),NUNO(I),RENO,PRND	900
ISN 0194	114	FORMAT (IHO,9F13.4)	910
ISN 0195	115	CONTINUE	920
ISN 0196		HAVG=AVG(H,FTC,CTC,X1,X2)	930
ISN 0197		PRINT 450,HAvg	935
ISN 0198	450	FORMAT (IHO,'AVG H BTU/HR SQFT DEG F = ',F10.2)	940
ISN 0199		HAvg=AVG(TI,FTC,CTC,X1,X2)	950
ISN 0200		PRINT 451,HAvg	955
ISN 0201	451	FORMAT (IHO,'AVG INNER WALL TEMP DEG F = ',F10.3)	960
ISN 0202		BAvg=AVG(TB,FTC,CTC,X1,X2)	970
ISN 0203		PRINT 452,BAvg	975
ISN 0204	452	FORMAT (IHO,'AVG BULK TEMP DEG F = ',F10.3)	980
ISN 0205		CAvg=AVG(TO,FTC,CTC,X1,X2)	990
ISN 0206		PRINT 453,CAvg	995
ISN 0207	453	FORMAT (IHO,'AVG OUTER WALL TEMP DEG F = ',F10.3)	1000
ISN 0208		NUAVG=AVG(ALNO,FTC,CTC,X1,X2)	1005
ISN 0209		PRINT 454,NUAVG	1010
ISN 0210	454	FORMAT (IHC,'AVG NUSSELT NO. = ',F10.5)	1015
ISN 0211		CALL PROP(RENO,PRNC,PU,RHO,RAVG,R1,CCND,SPH1,MDOT)	1017
ISN 0212		VRAT=MU	1018
ISN 0213		BETA=0.02328/RHO	1019
ISN 0214		PRINT 90,QHM	1020A
ISN 0215	90	FORMAT (IHL,'WATTMETER BTU/HR = ',T35,F10.3)	1020B
ISN 0216		PRINT 91,QF	1020B1
ISN 0217	91	FORMAT (IHO,'HEAT TO SALT BTU/HR = ',T35,F10.3)	1020B2
ISN 0218		PRINT 93,QLCAL	1020C
ISN 0219	93	FORMAT (IHO,'CAL HEAT LOSS BTU/HR = ',T35,F10.3)	1020D
ISN 0220		PRINT 94,QLEST	1020E
ISN 0221	94	FORMAT (IHO,'EST HEAT LOSS BTU/HR = ',T35,F10.3)	1020F
ISN 0222		PRINT 96,N	1020I
ISN 0223	96	FORMAT (IHO,'TEST SECTION NO. = ',T35,I10)	1020J
ISN 0224		G=MDOT/(3.14*R1*R1)*144.	1020J3
		PRINT 97,G	1020J4
ISN 0225	C	97 FORMAT (IHO,'G LB/HR FT2 = ',T33,E12.5)	1020J5
ISN 0226		VEL=MDOT/RHO/(3.14*R1*R1/144.)/3600.	1020L1
		PRINT 98,VEL	1020L2
ISN 0227	C	98 FORMAT (IHO,'TEST VELOCITY FT/SEC = ',T35,F10.3)	1020L3
ISN 0228		PRINT 99,RHO	1050
ISN 0229	99	FORMAT (IHO,'BULK SALT DENSITY LB/FT3 = ',T35,F10.2)	1055
ISN 0230		PRINT 100,PU	1060
ISN 0231	100	FORMAT (IHC,'BULK SALT VISCOSITY LB/HR FT = ',T35,F10.3)	1065
ISN 0232		PRINT 101,COND	1080
ISN 0233	101	FORMAT (IHO,'BULK SALT COND BTU/HR FT DEG F = ',T35,F10.3)	1090
ISN 0234		PRINT 472,TIN	1110
ISN 0235	472	FORMAT (IHO,'INLET TEMP DEG F = ',T35,F10.3)	1120
ISN 0236		PRINT 473,TOUT	1130
ISN 0237	473	FORMAT (IHO,'OUTLET TEMP DEG F = ',T35,F10.3)	1140
ISN 0238		TCHG=TCUT-TIN	1150
ISN 0239		PRINT 474,TCHG	1160
ISN 0240	474	FORMAT (IHO,'TOUT - TIN DEG F = ',T35,F10.3)	1170
ISN 0241		PRINT 471,MDOT	1180
ISN 0242	471	FORMAT (IHO,'MASS FLOW RATE LB/HR = ',T35,F10.3)	1185
ISN 0243		PRINT 477,RENO	1190
ISN 0244	477	FORMAT (IHC,'BULK REYNOLDS NO. = ',T35,F10.2)	1200
ISN 0245		PRINT 478,PRND	1210
ISN 0246	478	FORMAT (IHC,'BULK PRANCTL NO. = ',T35,F10.3)	1220
ISN 0247		PRINT 470,COND	1230

ISN 0248	470	FORMAT (IHO, 'NET HEAT FLUX BTU/HR SOFT = ', T33, E12.5)	1235
ISN 0249		PRINT 476, CBAL	1240
ISN 0250	476	FORMAT (IHO, 'HEAT BALANCE = ', T35, F10.3)	1245
ISN 0251		DEFH=MDOT*SPH1*(TOUT-TIN)/(2.*3.14*R1*L/144.*(WAVG-BAVG))	1250
ISN 0252		PRINT 475, CEFH	1260
ISN 0253	475	FORMAT (IHI, 'H BY DEF BTU/HR SOFT DEGF = ', T35, F10.2)	1270
ISN 0254		NNO=DEFH*2.*R1/12./CCND	1290
ISN 0255		PRINT 4751, NNO	1291
ISN 0256	4751	FORMAT (IHO, 'NUSSELT NC. = ', T35, F10.2)	1292
		C FROM HERE ON THE NNO USED WILL BE THE INTEGRATED VALUE	1292A
ISN 0257		NNO=NUAVG	1292B
ISN 0258		GRNO= D1 **3*BETA*32.2*RHO**2*(WAVG-BAVG)/(MU/3600.)***2	1293
ISN 0259		PRINT 981, GRNO	1294
ISN 0260	981	FORMAT (IHO, 'GRASHOF NO. = ', T35, F10.4)	1295
ISN 0261		GZNO=3.14/4.*RENO*PRNO*2.*R1/(X2-X1)	1296
ISN 0262		PRINT 4752, GZNO	1297
ISN 0263	4752	FORMAT (IHO, 'GRAETZ NO. (P-B) = ', T35, F10.4)	1298
ISN 0264		BTRM=0.0722*(GRNO*PRNO*2.*R1/(X2-X1))*0.75	1299
ISN 0265		PRINT 4753, BTRM	1300
ISN 0266	4753	FORMAT (IHO, 'BUOYANCY TERM FOR VERT. LJM = ', T35, F10.4)	1301
ISN 0267		STF=NNO/(PRNO**0.33)/(MU**0.14)	1310
ISN 0268		DSF=NNO/PRNO**0.4	1320
ISN 0269		OBH=COND/(2.*R1/12.)*G.023*(RENO**0.8)*(PRNO**0.4)	1330
ISN 0270		PRINT 481, CBH	1340
ISN 0271	481	FORMAT (IHO, 'MC ADAMS H BTU/HR SOFT CEGF = ', T35, F10.2)	1350
ISN 0272		STTH=COND/(2.*R1/12.)*G.027*(RENO**0.8)*(PRNO**0.33)*(MU**0.14)	1355
ISN 0273		HTRH=COND/(2.*R1/12.)*0.116*(RENO**0.667 - 125.)*PRNO**0.33	1357
		*(MU**0.14)	1358
ISN 0274		STH=COND/(2.*R1/12.)*1.86*(RENO*PRNO*2.*R1/(X2-X1))*0.33	1360
ISN 0275		IF (TA-TBB) 200, 210, 210	1360A
ISN 0276	200	DLH=COND/D1*1.75*(GZNO - BTRM)**0.33	1360B
ISN 0277		GO TO 220	1360C
ISN 0278	210	DLH=COND/D1*1.75*(GZNO + BTRM)**0.33	1360D
ISN 0279	220	CONTINUE	1360E
ISN 0280		STH=STH*(ML**0.14)	1361
ISN 0281		COLH=0.023*(D1*G)**0.8/D1*CCND**0.667*SPH1**0.33	1361A
ISN 0282		CLMH=1.65*COND/D1*(GZNO*MU)**0.33	1361A00
ISN 0283		FGRNO=GRNO*MU**2	1361A0
ISN 0284		CF=NNO/(PRNO**0.33)*(MU**0.33)	1361A1
ISN 0285		FILM=(WAVG+BAVG)/2.	1361B
		C DIM GROUPS AND PROPS THAT FOLLOW ARE NO LONGER AT BULK TEMP	1361B1
ISN 0286		CALL PROP (RENO, PRNO, MU, RHO, FILM, R1, CCND, SPH1, MDOOT)	1361C
ISN 0287		COLH=COLH*MU**0.33/MU**0.8	1361D
ISN 0288		FGRNO=FGRNO/MU**2	11361D1
ISN 0289		IF (TA-TBB) 230, 240, 240	1361D2
ISN 0290	230	CLMH=CLMH/MU**0.33*(1. - 0.015*(FGRNO)**0.33)	1361D3
ISN 0291		GO TO 250	1361D4
ISN 0292	240	CLMH=CLMH/MU**0.33*(1. + 0.015*(FGRNO)**0.33)	1361D5
ISN 0293	250	CONTINUE	1361D6
ISN 0294		CF=CF/MU**0.33	1361D7
ISN 0295		CRENO=RENO	1361D8
ISN 0296		PRINT 4811, COLH	1361E
ISN 0297	4811	FORMAT (IHO, 'COLBURN TURB H BTU/HR SOFT DEGF = ', T35, F10.2)	1361F
ISN 0298		CALL PROP (RENO, PRNO, MU, RHO, WAVG, R1, CCND, SPH1, MDOOT)	1362
ISN 0299		STH=STH/(MU**0.14)	1362B
ISN 0300		HTRH=HTRH/(MU**0.14)	1362C
ISN 0301		STH=STH/(ML**0.14)	1363
ISN 0302		PRINT 482, STTH	1364

ISN 0303	482	FJRMAT(1HO,'S-T TURBULENT H BTU/HRSQFTDEGF = ',T35,F10.2)	1365
ISN 0304		PRINT 4821,HTRH	1366
ISN 0305	4821	FORMAT(1HO,'HAUSEN TR H BTU/HRSQFTDEGF = ',T35,F10.2)	1366A
ISN 0306		PRINT 483,STM	1367
ISN 0307	483	FORMAT(1HO,'S-T LAMINAR H BTU/HRSQFTCEGF = ',T35,F10.2)	1368
ISN 0308		PRINT 484,DLH	1369A
ISN 0309	484	FORMAT(1HO,'MART VER,LAM H BTU/HRSQFTCEGF = ',T35,F10.2)	1369B
ISN 0310		PRINT 4840,CLMH	1369B1
ISN 0311	4840	FORMAT(1HO,'COL VERT,LAM H BTU/HRSQFTDEGF = ',T35,F10.2)	1369B2
ISN 0312		PRINT 4841,DBF	1369C1
ISN 0313	4841	FORMAT(1HC,'MC ADAMS FACTOR = ',T35,F10.3)	1369C2
ISN 0314		PRINT 4842,CF	1369C3
ISN 0315	4842	FORMAT(1HO,'COLEBURN FACTOR = ',T35,F10.3)	1369C4
ISN 0316		PRINT 4843,CRENO	1369C5
ISN 0317	4843	FORMAT(1HO,'CLBRN RENC = ',T35,F10.2)	1369C6
ISN 0318		STF=STF*(HL**0.14)	1370A
ISN 0319		PRINT 485,STF	1370B
ISN 0320	485	FORMAT(1HO,'S-T FACTOR = ',T35,F10.3)	1370C
ISN 0321		ETL=X2-X1	1372
ISN 0322		PRINT 486,ETL	1373
ISN 0323	486	FORMAT(1HO,'EFF TUBE LENGTH IN = ',T35,F10.3)	1374
ISN 0324		VRAT=(VRAT/MUI)**0.14	1375
ISN 0325		PRINT 487,VRAT	1376
ISN 0326	487	FORMAT(1HO,'VIS RATIO TO 0.14 = ',T35,F10.4)	1377
ISN 0327		DFACT=STF*VRAT	1378
ISN 0328		PRINT 488,CFACT	1379
ISN 0329	488	FORMAT(1HO,'MART FACTOR = ',T35,F10.3)	1380
		C A LOOK AT A SMOOTH CURVE THRU THE DATA POINTS MAY BE EDUCATIONAL	1390
ISN 0330		CALL YLS(ITC,FTC,CTC,2)	1391
ISN 0331		GO TO 6	1400
ISN 0332		END	1401

AOCONS FOR EXTERNAL REFERENCES


```

COMPILER OPTIONS - NAME= MAIN,CPT=02,LINECNT=63,SOURCE,EBCDIC,NOLIST,DECK,LOAD,MAP,NOEDIT,NOID,NOXREF
C THIS FUNCTION COMPUTES 3RD ORDER ORTHOGONAL SINS BY AVERAGING VALUES
C BEGINNING WITH NO. M AT X1 AND ENDING WITH I CONSECUTIVE VALUES AT X2
ISN 0002      FUNCTION AVG(Y,M,I,X1,X2)
ISN 0003      DIMENSION Y(50),X(50),A(4),P(50,4),SP2(50,4)
ISN 0004      REAL NP,LS
ISN 0005      A(1)=0
ISN 0006      A(2)=0
ISN 0007      A(3)=0
ISN 0008      A(4)=0
ISN 0009      P(1,1)=1.
ISN 0010      P(1,2)=1.
ISN 0011      P(1,3)=1.
ISN 0012      P(1,4)=1.
ISN 0013      NP=I-1
ISN 0014      DO 490 L=2,I
ISN 0015      X(L)=L-1
ISN 0016      P(L,1)=1.
ISN 0017      P(L,2)=1.-2.*X(L)/NP
ISN 0018      P(L,3)=1.-6.*X(L)/NP+6.*X(L)*(X(L)-1.)/NP/(NP-1.)
ISN 0019      P(L,4)=1.-12.*X(L)/NP+30.*X(L)*(X(L)-1.)/NP/(NP-1.)
          9      -20.*X(L)*(X(L)-1.)*(X(L)-2.)/NP/(NP-1.)/(NP-2.)
ISN 0020      490 CONTINUE
ISN 0021      SP2(I,1)=NP+1.
ISN 0022      SP2(I,2)=(NP+1.)*(NP+2.)/(3.*NP)
ISN 0023      SP2(I,3)=(NP+1.)*(NP+2.)*(NP+3.)/(5.*NP)/(NP-1.)
ISN 0024      SP2(I,4)=(NP+1.)*(NP+2.)*(NP+3.)*(NP+4.)/(7.*NP)/(NP-1.)/(NP-2.)
ISN 0025      DO 550 J=1,4
ISN 0026      DO 500 K=1,I
ISN 0027      A(J)=A(J)+Y(K+M-1)*P(K,J)
ISN 0028      500 CONTINUE
ISN 0029      A(J)=A(J)/SP2(I,J)
ISN 0030      550 CONTINUE
ISN 0031      PRINT 600
ISN 0032      600 FORMAT (I1,10HORIGINAL ,13HLEAST SQUARES,10H      PDEV)
ISN 0033      DO 700 J=1,4
ISN 0034      LS=A(1)*P(J,1)+A(2)*P(J,2)+A(3)*P(J,3)+A(4)*P(J,4)
ISN 0035      PDEV=(LS-Y(J+M-1))*100./Y(J+M-1)
ISN 0036      PRINT 650,Y(J+M-1),LS,PDEV
ISN 0037      650 FORMAT (F8.2,5X,F8.2,5X,F8.2)
ISN 0038      700 CONTINUE
ISN 0039      X3=X2-X1
ISN 0040      750 AINT=A(1)*X3 + A(2)*(X3-X3**2/NP) +
          8      A(3)*(X3-3.*X3**2/NP+6./NP/(NP-1.))*(X3**3/3.-X3**2
          8      /2.) +
          8      A(4)*(X3-6.*X3**2/NP+30./NP/(NP-1.))*(X3**3/3.-X3**2
          8      /2.)-20./NP/(NP-1.)/(NP-2.)*(X3**4/4.-X3**3*X3*X3)
ISN 0041      AVG=AINT/X3
ISN 0042      RETURN
ISN 0043      END

```

A10
A11
A20
A30
A35
A40
A50
A60
A70
A72
A73
A74
A75
A90
A95
A97
A100
A110
A120
A130
A131
A135
A140
A150
A160
A170
A200
A210
A220
A230
A240
A250
A270
A280
A290
A300
A305
A310
A320
A330
A340
A350
A351
A352
A353
A354
A390
A440
A450

COMPILER OPTIONS - NAME= MAIN,CPT=02,LINECNT=60,SOURCE,EBCDIC,NOLIST,DECK,LOAD,MAP,NOEDIT,NOID,NOXREF

```
C THIS FUNCTION DETERMINES THERMAL K FOR INCR-8
FUNCTION TK(TEMPF)
K10
K20
TEMPC=(TEMPF-32.)*5./9.
K30
IF (TEMPC-440.)10,10,20
K40
10 TK=0.128+(.155-.128)/200.*(TEMPC-200.)
K50
ISN 0006 GO TO 80
K60
ISN 0007 20 IF (TEMPC-500.)30,30,40
K70
ISN 0008 30 TK=0.160+(.174-.160)/60.*(TEMPC-440.)
K80
ISN 0009 GO TO 80
K90
ISN 0010 40 IF (TEMPC-680.)50,50,60
K100
ISN 0011 50 TK=0.174+(.193-.174)/100.*(TEMPC-500.)
K110
ISN 0012 GO TO 80
K120
ISN 0013 60 IF (TEMPC-740.)70,70,75
K130
ISN 0014 70 TK=0.208+(.230-.208)/60.*(TEMPC-680.)
K140
ISN 0015 GO TO 80
K150
ISN 0016 75 TK=0.230+(.248-.230)/160.*(TEMPC-740.)
K160
ISN 0017 80 TK=TK*57.82
K170
ISN 0018 RETURN
K300
ISN 0019 END
K301
```

```

COMPILER OPTIONS - NAME= MAIN,OPT=02,LINECNT=60,SOURCE,EBCDIC,NOLIST,DECK,LOAD,MAP,NOEDIT,NCIC,NOXREF
C THIS SUBROUTINE TAKES AN ARRAY Y WHCSE 1ST VALUE IS AT M WITH I TOTAL
C CONSECUTIVE VALUES AND REPLACES THIS ARRAY WITH AN NTH ORDER FIT
ISN 0002      SUBROUTINE YLS(Y,M,I,N)
ISN 0003      DIMENSION Y(50),X(50),A(4),P(50,4),SP2(50,4)
ISN 0004      REAL NP,LS
ISN 0005      A(1)=0
ISN 0006      A(2)=0
ISN 0007      A(3)=0
ISN 0008      A(4)=0
ISN 0009      P(1,1)=1.
ISN 0010      P(1,2)=1.
ISN 0011      P(1,3)=1.
ISN 0012      P(1,4)=1.
ISN 0013      NP=I-1
ISN 0014      DO 490 L=2,I
ISN 0015      X(L)=L-1
ISN 0016      P(L,1)= 1.
ISN 0017      P(L,2)=1.-2.*X(L)/NP
ISN 0018      P(L,3)=1.-6.*X(L)/NP+5*X(L)*(X(L)-1)/NP/(NP-1.)
ISN 0019      P(L,4)=1.-12.*X(L)/NP+30.*X(L)*(X(L)-1)/NP/(NP-1.)
                8      -20.*X(L)*(X(L)-1.)*(X(L)-2.)/NP/(NP-1.)/(NP-2.)
ISN 0020      490 CONTINUE
ISN 0021      SP2(I,1)=NP+1.
ISN 0022      SP2(I,2)=(NP+1.)*(NP+2.)/(3.*NP)
ISN 0023      SP2(I,3)=(NP+1.)*(NP+2.)*(NP+3.)/(5.*NP)/(NP-1.)
ISN 0024      SP2(I,4)=(NP+1.)*(NP+2.)*(NP+3.)*(NP+4.)/(7.*NP)/(NP-1.)/(NP-2.)
ISN 0025      DO 550 J=1,4
ISN 0026      DO 500 K=1,I
ISN 0027      A(J)=A(J)+Y(K+M-1)*P(K,J)
ISN 0028      500 CONTINUE
ISN 0029      A(J)=A(J)/SP2(I,J)
ISN 0030      550 CONTINUE
ISN 0031      PRINT 600
ISN 0032      600 FORMAT (1H1,10HORIGINAL ,13HLEAST SQUARES,10H      PDEV)
ISN 0033      DO 700 J=1,I
ISN 0034      IF (N.LT.3) A(4)=0
ISN 0035      IF (N.LT.2) A(3)=0
ISN 0036      IF (N.LT.1) A(2)=0
ISN 0040      LS=A(1)*P(J,1)+A(2)*P(J,2)+A(3)*P(J,3)+A(4)*P(J,4)
ISN 0041      PDEV=(LS-Y(J+M-1))*100./Y(J+M-1)
ISN 0042      PRINT 650,Y(J+M-1),LS,PDEV
ISN 0043      650 FORMAT (F8.2,5X,F8.2,5X,F8.2)
ISN 0044      Y(J+M-1)=LS
ISN 0045      700 CONTINUE
ISN 0046      RETURN
ISN 0047      END

```

A10
A11
A20
A30
A35
A40
A50
A60
A70
A72
A73
A74
A75
A90
A95
A97
A100
A110
A120
A130
A131
A135
A140
A150
A160
A170
A200
A210
A220
A230
A240
A250
A270
A280
A290
A294
A295
A296
A300
A305
A310
A320
A330
A350
A370
A371

```

COMPILER OPTIONS - NAME= MAIN,OPT=02,LINECNT=60,SIZE=0000K,
SOURCE,EBCDIC,NOLIST,NODECK,LOAD,MAP,NOEDIT,NOID,NOXREF
C THIS SUBROUTINE USES THERMOPHYSICAL DATA FROM ORNL-TM-2316 AND ORNL-4449
ISN 0002 SUBROUTINE PROP(RE,PR,V,RHO,TEMPF,R,COND,CP,W) P20
ISN 0003 T=(TEMPF-32.0)/1.8
ISN 0004 V=T+273.0
ISN 0005 V=0.077*EXP(4430.0/T)
ISN 0006 V=2.419*V
ISN 0007 RHO=3.687-(6.5E-04*T)
ISN 0008 RHO=RHO*62.428
ISN 0009 COND=0.69
ISN 0010 PR=CP*V/COND P140
ISN 0011 RE=4./V/3.14/(2.*R/12.)*W P150
ISN 0012 RETURN P199
ISN 0013 END P200

```

APPENDIX D

CHEMICAL ANALYSES AND PHYSICAL PROPERTIES OF THE SALT

C

C

Table D.1. Analyses of the Fluoride Salt Mixture
 (LiF-BeF₂-ThF₄-UF₄; 67.5-20.0-12.0-0.5 mole %)
 Before, During, and After Heat-
 Transfer Determinations

Impurity	Weight %		
	Before	During ^a	After
Li	7.14	7.27	6.64
Be	2.57	2.53	2.46
Th	42.1	41.3	43.5
U	1.87	1.84	1.72
F	45.4	46.4	45.4
Ni	20 ppm	-	-
Cr	<25 ppm	-	-
Fe	78 ppm	-	-
S	<10 ppm	-	-
Na	-	0.66	0.55

^aAnalysis made just prior to removal of the first test section.

Table D.2. Thermophysical Property Data for Molten Salt
Mixture $\text{LiF}-\text{BeF}_2-\text{ThF}_4-\text{UF}_4$ (67.5-20-12-0.5 Mole %)

	Uncertainty	Ref.
μ (lb/ft·hr) = $0.187 \exp [8000/T(^{\circ}\text{R})]^a$	$\pm 25\%$	12
k (Btu/hr·ft· $^{\circ}\text{F}$) = 0.69^b	$\pm 12\%$	13
ρ (lb/ft ³) = $230.89 - 22.54 \times 10^{-3} t (^{\circ}\text{F})^a$	$\pm 3\%$	12
C_p (Btu/lb· $^{\circ}\text{F}$) = 0.324^a	$\pm 4\%$	12
Liquidus temperature $\cong 895^{\circ}\text{F}^a$	$\pm 10^{\circ}\text{F}$	12

^aEstimated values for the salt mixture $\text{LiF}-\text{BeF}_2-\text{ThF}_4-\text{UF}_4$ (68-20-11.7-0.3 mole %).

^bMeasured value for the subject salt mixture.

INTERNAL DISTRIBUTION

- | | | | |
|--------|----------------------|----------|----------------------------------|
| 1. | L. B. Alexander | 63. | J. W. Krewson |
| 2. | J. L. Anderson | 64. | C. G. Lawson |
| 3. | S. E. Beall | 65. | M. I. Lundin |
| 4. | M. Bender | 66. | R. N. Lyon |
| 5. | E. S. Bettis | 67. | H. G. MacPherson |
| 6. | E. G. Bohlmann | 68. | R. E. MacPherson |
| 7. | C. J. Borkowski | 69. | H. E. McCoy |
| 8. | C. E. Boyd | 70. | H. C. McCurdy |
| 9. | R. B. Briggs | 71. | D. L. McElroy |
| 10. | R. H. Chapman | 72. | H. A. McLain |
| 11. | S. J. Claiborne, Jr. | 73. | L. E. McNeese |
| 12-21. | J. W. Cooke | 74. | J. R. McWherter |
| 22. | W. B. Cottrell | 75. | A. S. Meyer |
| 23-27. | B. Cox (K-25) | 76. | A. J. Miller |
| 28. | F. L. Culler | 77. | S. L. Milora |
| 29. | J. H. DeVan | 78. | W. R. Mixon |
| 30. | J. R. DiStefano | 79. | R. L. Moore |
| 31. | S. J. Ditto | 80. | A. M. Perry |
| 32. | A. S. Dworkin | 81. | J. Pidkowicz |
| 33. | W. P. Eatherly | 82-83. | M. W. Rosenthal |
| 34. | D. M. Eissenberg | 84. | W. K. Sartory |
| 35. | J. R. Engel | 85. | Dunlap Scott |
| 36. | D. E. Ferguson | 86. | J. H. Shaffer |
| 37. | L. M. Ferris | 87. | Myrtlelen Sheldon |
| 38. | A. P. Fraas | 88. | J. D. Sheppard |
| 39. | J. H. Frye | 89. | M. J. Skinner |
| 40. | C. H. Gabbard | 90. | I. Spiewak |
| 41. | R. B. Gallaher | 91. | D. A. Sunberg |
| 42. | W. R. Gambill | 92. | R. E. Thoma |
| 43. | R. H. Guymon | 93. | D. G. Thomas |
| 44. | P. N. Haubenreich | 94. | D. B. Trauger |
| 45. | R. B. Heimdahl | 95. | J. R. Weir |
| 46-55. | H. W. Hoffman | 96. | G. D. Whitman |
| 56. | W. R. Huntley | 97. | R. P. Wichner |
| 57. | P. R. Kasten | 98. | M. K. Wilkinson |
| 58. | R. J. Kedl | 99. | A. M. Weinberg |
| 59. | J. J. Keyes, Jr. | 100-102. | Central Research |
| 60. | O. H. Klepper | 103. | Y-12 Document Reference Section |
| 61. | A. I. Krakoviak | 104-105. | Laboratory Records |
| 62. | T. S. Kress | 106. | Laboratory Records - Record Copy |

EXTERNAL DISTRIBUTION

- 107. Branch Chief, Special Technology, RDT, USAEC, Washington, DC 20545
- 108. Director, Division of Reactor Development and Technology, USAEC, Washington, DC 20545
- 109-111. Director, Division of Reactor Licensing, USAEC, Washington, DC 20545
- 112-113. Director, Division of Reactor Standards, USAEC, Washington, DC 20545
- 114-130. Manager, Technical Information Center, USAEC (For ACRS Members)
- 131-132. MSBR Program Manager, USAEC, Washington, DC 20545
- 133. Research and Technical Support Division, USAEC, ORO
- 134-135. Technical Information Center, USAEC
- 136. D. F. Cope, RDT Site Office, ORNL
- 137. A. R. DeGrazia, USAEC, Washington, DC 20545
- 138-139. Norton Haberman, USAEC, Washington, DC 20545
- 140. Kermit Laughton, RDT Site Office, ORNL